

Topo-Bathymetric Lidar and Photographic Survey of Various Bays located in New Brunswick, Nova Scotia and Prince Edward Island



Prepared by



Kate Collins, Tim Webster, PhD, Nathan
Crowell, Kevin McGuigan, Candace
MacDonald
Applied Geomatics Research Group
NSCC, Middleton
Tel. 902 825 5475
email: tim.webster@nsc.ca

Submitted to



Marc Ouellette
Fisheries and Oceans Canada
Gulf Region

March 30, 2016

Topo-Bathymetric Lidar and Photographic Survey of Various Bays located in NB, NS, and PEI

How to cite this work and report:

Collins, K., Webster, T., Crowell, N., McGuigan, K., MacDonald, C. 2016. Topo-Bathymetric Lidar and Photographic Survey of Various Bays located in NB, NS, and PEI. Technical report, Applied Geomatics Research Group, NSCC Middleton, NS.

Copyright and Acknowledgement

The Applied Geomatics Research Group of the Nova Scotia Community College maintains full ownership of all data collected by equipment owned by NSCC and agrees to provide the end user who commissions the data collection a license to use the data for the purpose they were collected for upon written consent by AGRG-NSCC. The end user may make unlimited copies of the data for internal use; derive products from the data, release graphics and hardcopy with the copyright acknowledgement of **“Data acquired and processed by the Applied Geomatics Research Group, NSCC”**. Data acquired using this technology and the intellectual property (IP) associated with processing these data are owned by AGRG/NSCC and data will not be shared without permission of AGRG/NSCC.

Executive Summary

Three topographic-bathymetric lidar and photographic surveys were conducted in bay areas around the southern Gulf of St. Lawrence, New Brunswick (NB), in the fall of 2015. Digital Elevation Models (DEMs), Digital Surface Models (DSMs), Colour Shaded Relief models (CSRs), Depth Normalized Intensity models (DNI), and ortho-rectified aerial photograph mosaics were generated for each study site.

Saint-Simon is a shallow estuary in northern NB and was surveyed on October 24, 2015. Lidar collection was successful and penetration was achieved throughout the study area except for a wide, deep channel; minimum seabed elevation was -5.1 m near the edge of the channel, referenced to the Canadian Geodetic Vertical Datum of 1928 (CGVD28). The photographic survey of Saint-Simon revealed aquaculture floating on the surface and submerged vegetation throughout the bay.

Tabusintac Bay, NB, is a shallow, eelgrass-containing bay north of Miramichi, NB. The northern portion of Tabusintac Bay was surveyed on October 26, 2015 but water quality was poor because of a northwest wind that induced waves which stirred up bottom sediment. The lidar data products suffered from lack of water column penetration. A second survey was completed on November 10, 2015 when wind conditions were improved, and the photographic and lidar products were improved. Unfortunately, this survey was aborted about two thirds of the way through the survey due to a problem with the lidar system. The final DEM is a synthesis of the two surveys referenced to a local Chart Datum (CD), and the minimum seabed elevation achieved by the lidar was -5.75 m CD outside of the bay; good data coverage within the bay was achieved, excepting the deep channel, and depths within the bay ranged from 1.5 m CD to -0.2 m CD. The photographic surveys at Tabusintac revealed floating aquaculture on Oct. 26, but by Nov. 10 most of the aquaculture was removed from the surface. Submerged vegetation can be seen in the aerial photographs.

A third survey was completed of Cocagne River, NB, east of Moncton, NB, on October 22, 2015. The study area built upon a 2014 lidar survey of the Cocagne Harbour by AGRG. As with Saint-Simon and Tabusintac, the survey of Cocagne River achieved excellent lidar coverage outside of the channel, with a maximum lidar penetration at Cocagne of -2.6 m CGVD28 near the mouth of the river.

Ground truth surveys were conducted during the lidar surveys at each study area. The topographic ground truth consisted of collecting elevation data on hard, flat surfaces; mean differences between the survey elevations and the DEMs were 0.11 m, 0.20 m, and -0.05 m at Saint-Simon, Tabusintac, and Cocagne, respectively. The

Topo-Bathymetric Lidar and Photographic Survey of Various Bays located in NB, NS, and PEI boat-based bathymetric ground truth surveys consisted of depth measurements to validate the lidar, Secchi depth measurements for information on water clarity, and underwater photographs to obtain information on bottom type and vegetation. Mean differences between the depth measurements, which were direct measurements of the seabed using high precision GPS, and the DEMs were -0.22 m, -0.23 m, and -0.27 m, for Saint-Simon, Tabusintac, and Cocagne, respectively. These negative numbers indicate that the DEMs were shallower than the survey points of the seabed, an indication that the lidar did not penetrate to the bottom. A possible explanation for this is the presence of a thick eelgrass canopy of approximately 0.20 m that attenuated the laser pulse. Light sensors were deployed in Saint-Simon and Tabusintac approximately one month prior to the lidar survey to provide information on water clarity as it related to wind speed and direction.

Table of Contents

Executive Summary.....	ii
Table of Contents.....	iv
Table of Figures.....	vi
List of Tables.....	ix
1 Introduction.....	1
1.1 Study Area.....	1
2 Methods.....	2
2.1 Sensor Specifications and Installation.....	2
2.2 Lidar Survey Details.....	4
2.3 Ground Truth Data Collection.....	5
2.3.1 Light Sensors.....	7
2.3.2 Vegetation Ground Truth.....	8
2.4 Meteorological, Light and Tidal Conditions.....	14
2.4.1 Meteorology.....	14
2.4.2 Tide.....	17
2.4.3 Light.....	18
2.5 Elevation Data Processing.....	19
2.5.1 Lidar processing.....	19
2.5.2 Ellipsoidal to Orthometric Height Conversion.....	21
2.6 Lidar Validation.....	22
3 Results.....	22
3.1 Lidar Validation.....	22
3.1.1 Topographic Validation.....	22
3.1.2 Bathymetric Validation.....	23
3.2 Surface Models.....	26
3.2.1 Digital Elevation Models.....	26

Topo-Bathymetric Lidar and Photographic Survey of Various Bays located in NB, NS, and PEI

3.2.2 Colour Shaded Relief Models 28

3.2.3 Normalized Intensity Models 31

3.3 Air Photos 34

4 Discussion 39

4.1 Merging 2014 and 2014 Datasets 39

5 Conclusions 42

6 References 43

7 Acknowledgements 43

Table of Figures

Figure 1.1: The topographic-bathymetric lidar study areas in the Southern Gulf of St. Lawrence surveyed in 2014 (blue) and 2015 (red) showing base stations (NB high precision network stations and a CHS benchmark, orange squares) and Environment Canada Weather Stations (green triangles)..... 2

Figure 2.1: (A) Example of the Chiroptera II green laser waveform showing the large return from the sea surface and smaller return from the seabed. (B) Schematic of the Chiroptera II green and NIR lasers interaction with the sea surface and seabed (adapted from Leica Geosystems)..... 3

Figure 2.2: (a) Aircraft used for 2015 lidar survey; (b) display seen by lidar operator in-flight; (c) main body of sensor (right) and the data rack(left); (d) large red circles are the lasers; the RCD30 lens (right) and low resolution camera quality control(left)..... 4

Figure 2.3: Flight lines planned for the 2015 study areas (A) Saint-Simon Bay, (B) Tabusintac Bay North, and (C) Cocagne River..... 5

Figure 2.4: Ground truth images (a) GPS base station set up over HPN monument at Cocagne; (b) RTK GPS depth measurement using pole; (c) submerged Secchi disk; (d) Seaviewer underwater video camera; (e) 0.25 m² quadrat being deployed; (f) eelgrass at Tabusintac as photographed using quadrat..... 6

Figure 2.5: Location of hard surface GPS validation points, underwater and onshore light sensors, and boat-based ground truth waypoints at (A) Saint-Simon, (B) Tabusintac, and (C) Cocagne River. Note that no light sensors were deployed in Cocagne River, and there were no roads in the Tabusintac North study area for hard surface validation. 7

Figure 2.6: (a) A single light sensor secured to a cinder block (not used in PARR study areas); (b,d) underwater photo of cinder block and light sensor deployment at Tabusintac (b) and Saint Simon (d); (c) the light sensors after being retrieved from Tabusintac Bay in October..... 8

Figure 2.7: Saint Simon underwater photo ground truth on (a) October 9 and (b) October 24. N/A indicates no underwater photograph was taken, or the visibility was too poor to assess eelgrass presence. Background image is RCD30 orthophoto RGB mosaic..... 10

Figure 2.8: Tabusintac underwater photo ground truth on (a) October 26 and (b) November 10. N/A indicates no underwater photograph was taken, or the visibility was too poor to assess eelgrass presence. 11

Figure 2.9: Tabusintac underwater video ground truth on October 7. Orange and red boxes are zoomed in on the transect at the center of the bay for eelgrass and water quality, respectively..... 12

Figure 2.10: Cocagne River underwater photo ground truth on (a) October 8 and (b) October 22. N/A indicates no underwater photograph was taken, or the visibility was too poor to assess eelgrass presence. Background image is RCD30 orthophoto RGB mosaic..... 13

Topo-Bathymetric Lidar and Photographic Survey of Various Bays located in NB, NS, and PEI

Figure 2.11: Wind speed (top panel) and direction (middle panel) collected at the EC weather station at Bas Caraquet between October 15 and November 14, 2015 at 1 hour intervals. The lower panel shows a stick plot of the wind, where the sticks point in the direction the wind is blowing, and the boxes indicates the lidar surveys (blue = Saint-Simon, red = Tabusintac Survey 1, green = Tabusintac Surey 2).	15
Figure 2.12: Wind speed (top panel) and direction (middle panel) collected at the EC weather station at Miramichi, NB between October 15 and November 14, 2015 at 1 hour intervals. The lower panel shows a stick plot of the wind, where the sticks point in the direction the wind is blowing, and the boxes indicates the lidar surveys (orange = Cocagne, red = Tabusintac Survey 1, green = Tabusintac Surey 2).....	16
Figure 2.13: (a,b,c) Conditions at Tabusintac on October 26, where wind caused rough seas and reduced water clarity. (d) shows improved conditions on November 10 during the second survey.	16
Figure 2.14: Tides for surveys at (a) Saint-Simon; (b) Tabusintac Survey 1; (c) Tabusintac Survey 2; (d) Cocagne. Grey bars indicate daylight hours and red boxes indicate survey durations.	17
Figure 2.15: Light sensor data at (a) Saint-Simon North and (b) Tabusintac. The % of underwater light is underwater light divided by onshore light. Red boxes indicate lidar survey dates. The blue lines are an average of the two sensors which were placed on each cinder block.....	18
Figure 3.1: Topographic lidar validation for (a) Saint-Simon, (b) Tabusintac, and (c) Cocagne.....	23
Figure 3.2: Bathymetric validation at (a) Saint-Simon; (b) Tabusintac; (c) Cocagne.	24
Figure 3.3: Saint Simon Bathymetry validation.....	24
Figure 3.4: Tabusintac Bathymetric Validation.....	25
Figure 3.5: Cocagne Bathymetric Validation.....	25
Figure 3.6: Saint Simon Digital Elevation Model for entire study area and insets beside which are matched to the larger figure by border colour.	26
Figure 3.7: Tabusintac Digital Elevation Model for entire study area and insets beside which are matched to the larger figure by border colour. The DEM is a synthesis of the two surveys (Oct. 26 and Nov 10).....	27
Figure 3.8: Cocagne River Digital Elevation Model for entire study area and insets beside which are matched to the larger figure by border colour.	28
Figure 3.9: Saint-Simon Bay bare-earth Colour Shaded Releif Model showing the whole study area, and insets beside which are matched to the larger figure by border colour.....	29
Figure 3.10: Tabusintac Bay bare-earth North Colour Shaded Releif Model showing the whole study area, and insets beside which are matched to the larger figure by border colour.	30
Figure 3.11: Cocagne River bare-earth Colour Shaded Releif Model showing the whole study area, and insets below which are matched to the larger figure by border colour.....	31

Topo-Bathymetric Lidar and Photographic Survey of Various Bays located in NB, NS, and PEI

Figure 3.12: Depth normalized intensity/amplitude for Saint-Simon, Oct. 24. The insets on the right corresepond to boxes of matching colour on the large map. The red and yellow insets highlight the different intensity signal for submerged eelgrass and sand, while the aqua inset shows floating (on the left) and submerged (on the right) aquaculture cages (the othophoto for this panel is shown in Figure 3.15).	32
Figure 3.13: Depth normalized intensity/amplitude for Tabusintac. The insets on the right corresepond to boxes of matching colour on the large map. The DNI is a sysnthesis of the two surveys (Oct. 26 and Nov 10).	33
Figure 3.14: Depth normalized intensity/amplitude for Cocagne, Oct. 22. The insets on the bottom corresepond to boxes of matching colour on the large map.	34
Figure 3.15: Saint-Simon Bay Orthophoto Mosaic from Oct. 24, 2015 showing the whole study area, and insets beside which are matched to the larger figure by border colour. The insets, from top to bottom, highlight submerged vegetation, the AGRG boat conducting ground truth surveys during the survey, and aquaculture, both submerged and floating, in the southern part of the bay (same extent as Figure 3.12).	35
Figure 3.16: Tabusintac Bay North Oct. 26 Orthophoto Mosaic showing the whole study area, and insets beside which are matched to the larger figure by border colour.	36
Figure 3.17: Tabusintac Bay North Nov. 10 Orthophoto Mosaic showing the whole study area, and insets beside which are matched to the larger figure by border colour. Note the absence of the aquaculture that was visible in Figure 3.16.	37
Figure 3.18: Cocagne River True Colour Composite Orthophoto Mosaic showing the whole study area, and insets below which are matched to the larger figure by border colour.	38
Figure 3.19: Photo products at Cocagne River showing the unenhanced orthophoto mosaic on the left, the enhanced true colour composite in the middle, and the near infrared image on the right. Note how the enhanced images (TCC and NIR) both show the submerged vegetation in much greater contrast and detail than the unenhanced photo.	38
Figure 4.1: Study areas for Tabusintac North, which was surveyed in 2015 for this project, and Tabusintac South, which was surveyed in 2014 for a PWGSC project.	39
Figure 4.2: Study areas for Cocagne River, which was surveyed in 2015 for this project, and Cocagne Harbour, which was surveyed in 2014, also for DFO Gulf Region.	40
Figure 4.3: Tabusintac North, which was surveyed in 2015 for this project, and Tabusintac South, which was surveyed in 2014 for a PWGSC project.	41
Figure 4.4: Study areas for Cocagne River, which was surveyed in 2015 for this project, and Cocagne Harbour, which was surveyed in 2014, also for DFO Gulf Region.	42

List of Tables

Table 1: 2015 lidar survey dates. 4

Table 2: Ground truth data summary. * Indicates that the ground truth survey was occurring simultanesouly with the lidar survey. GPS Column: Two Leica GPS systems were used the GS14 and the 530. Depth Column: P=GPS antenna threaded onto the large pole for direct bottom elevation measurement; M=manual depth measurement using lead ball or weighted Secchi disk; DM=handheld single beam DepthMate echo sounder; ES=Single beam commercial grade Humminbird Echo Sounder. Underwater Photos: P=GoPro camera secured to pole for underwater still photos; Q₅₀=0.25 m² quadrat with downward-looking GoPro camera; SV=SeaViewer underwater video camera..... 6

Table 3. Lidar point classification Codes and descriptions. Note that ‘overlap’ is determined for points which are within a desired footprint of points from a separate flight line; the latter of which having less absolute range to the laser sensor..... 20

1 Introduction

The Program for Aquaculture Regulatory Research (PARR) is a government program that supports the successful development of the Canadian aquaculture industry. This data presented here are part of a larger PARR-funded study entitled “The effect of cultured filter feeders on eelgrass productivity in estuaries of NB and PEI” which is being led by researchers at Fisheries and Oceans Canada in the Gulf Region in Moncton, NB. In 2015 the Applied Geomatics Research Group (AGRG) at the Nova Scotia Community College (NSCC) surveyed three bays in NB using a topographic-bathymetric lidar sensor equipped with a high resolution camera to complete the objectives of this study, “Topo-Bathymetric Lidar and Photographic Survey of Various Bays located in NB, NS, and PEI”. The data products resulting from the surveys will be used by researchers as part of the PARR project to investigate the relationship between eelgrass, depth, and aquaculture in the bays in order to sustainably manage and grow the aquaculture industry in NB, NS, and PEI.

This report outlines the Study Area below, describes the lidar sensor and camera in Section 2.1 and the lidar survey details in Section 2.2. The methods used for ground truth data collection, which included underwater photography, depth and water clarity measurements, are described in detail in Section 2.3, and many of the ground truth data and other supplementary data such as meteorological conditions and tides are presented in 2.4. The lidar and aerial photograph processing procedures are outlined in Section 2.5, and the methods for validating both the topographic and bathymetric lidar elevations are described in Section 2.6. Section 3 presents results of the lidar validation (Section 3.1), the surface models (Section 3.2), and the air photos (Section 0). Discussion and Conclusion follow, and two separate reports are delivered detailing the calibration of the sensor and the camera, and a Data Dictionary.

1.1 Study Area

The 2015 topographic-bathymetric lidar study areas built upon the areas completed in 2014 in the Southern Gulf of St. Lawrence region (Figure 1.1) and added a new area. Tabusintac Bay South was completed in 2014 for Public Works and Government Services Canada (PWGSC) and in 2015 the northern portion of the bay was surveyed for this project; Cocagne Harbour was surveyed in 2014 and in 2015 the river portion of the estuary was surveyed; Saint-Simon Bay North and South were both surveyed in 2015. These areas are all shallow inlets containing both eelgrass and shellfish aquaculture.

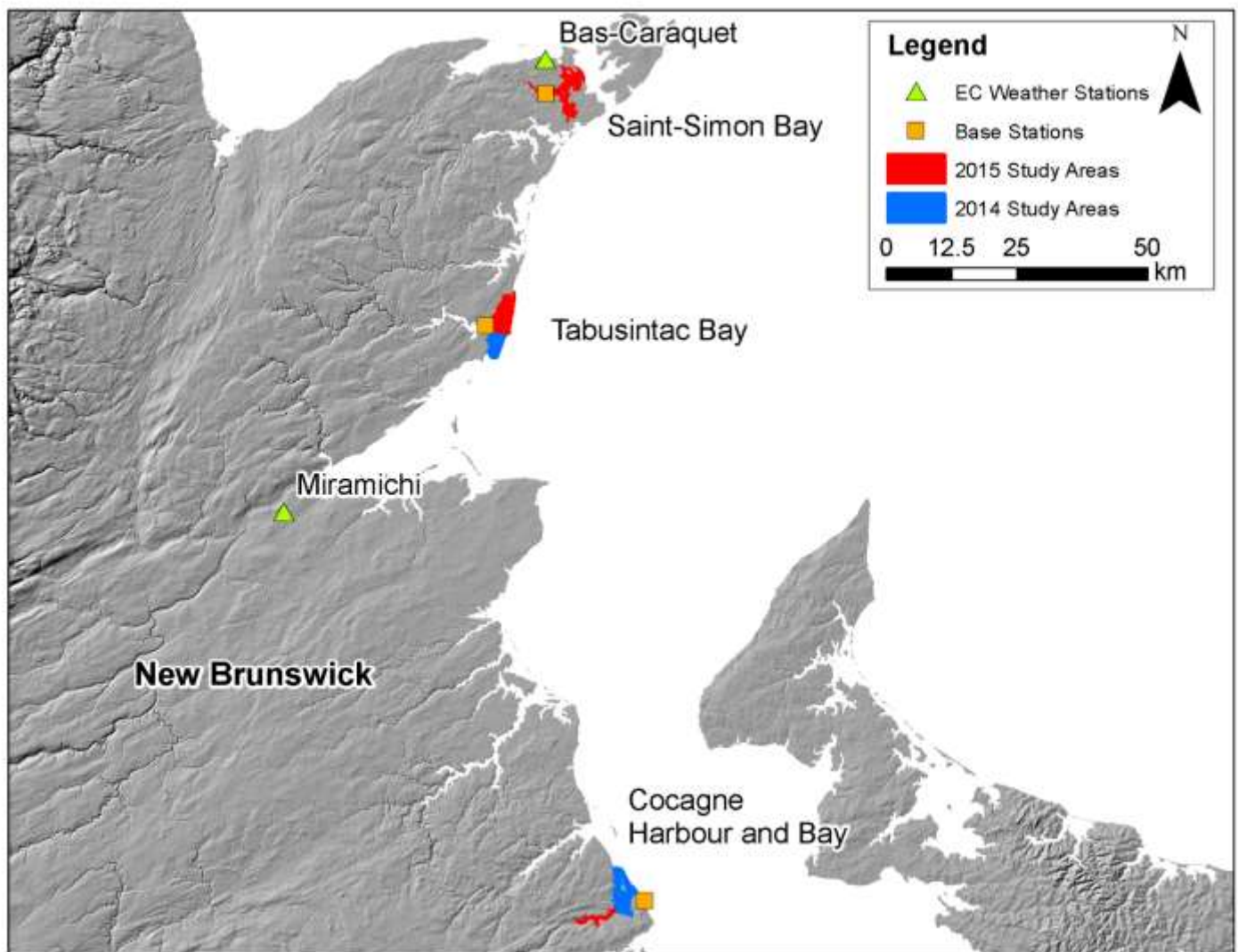


Figure 1.1: The topographic-bathymetric lidar study areas in the Southern Gulf of St. Lawrence surveyed in 2014 (blue) and 2015 (red) showing base stations (NB high precision network stations and a CHS benchmark, orange squares) and Environment Canada Weather Stations (green triangles).

2 Methods

2.1 Sensor Specifications and Installation

The lidar sensor used in this study is a Chiroptera II integrated topographic-bathymetric lidar sensor equipped with a 60 megapixel multispectral camera. The system incorporates a 1064 nm near-infrared laser for ground returns and sea surface and a green 515 nm laser for bathymetric returns (Figure 2.1). The lasers scan in an elliptical pattern, which enables coverage from many different angles on vertical faces, causes less shadow effects in the data, and is less sensitive to wave interaction. The bathymetric laser is limited by depth and clarity, and has a depth penetration rating of roughly 1.5 x the Secchi depth (a measure of turbidity or water clarity using a black and white disk). The Leica RCD30

Topo-Bathymetric Lidar and Photographic Survey of Various Bays located in NB, NS, and PEI camera collects co-aligned RGB+NIR motion compensated photographs which can be mosaicked into a single image in post-processing, or analyzed frame by frame for maximum information extraction.

The calibration of the lidar sensor and camera have been documented in an external report which is included as part of the deliverables for this project.

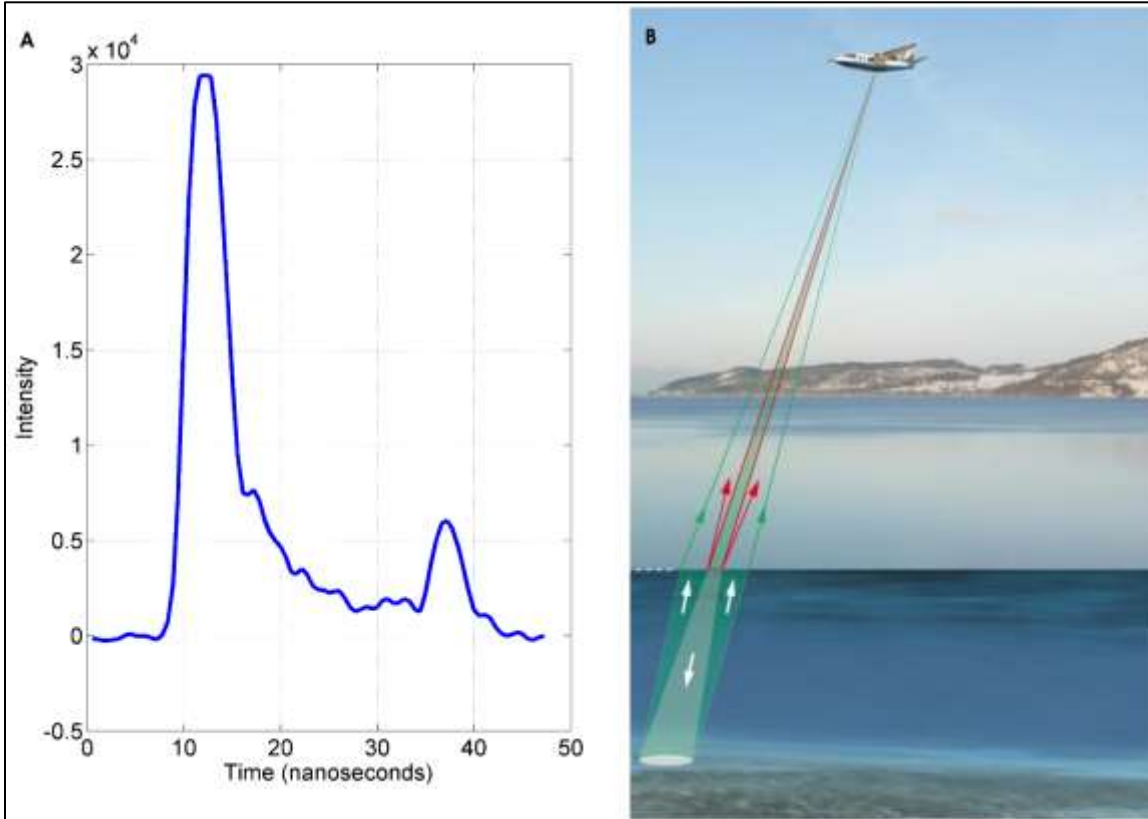


Figure 2.1: (A) Example of the Chiroptera II green laser waveform showing the large return from the sea surface and smaller return from the seabed. (B) Schematic of the Chiroptera II green and NIR lasers interaction with the sea surface and seabed (adapted from Leica Geosystems).

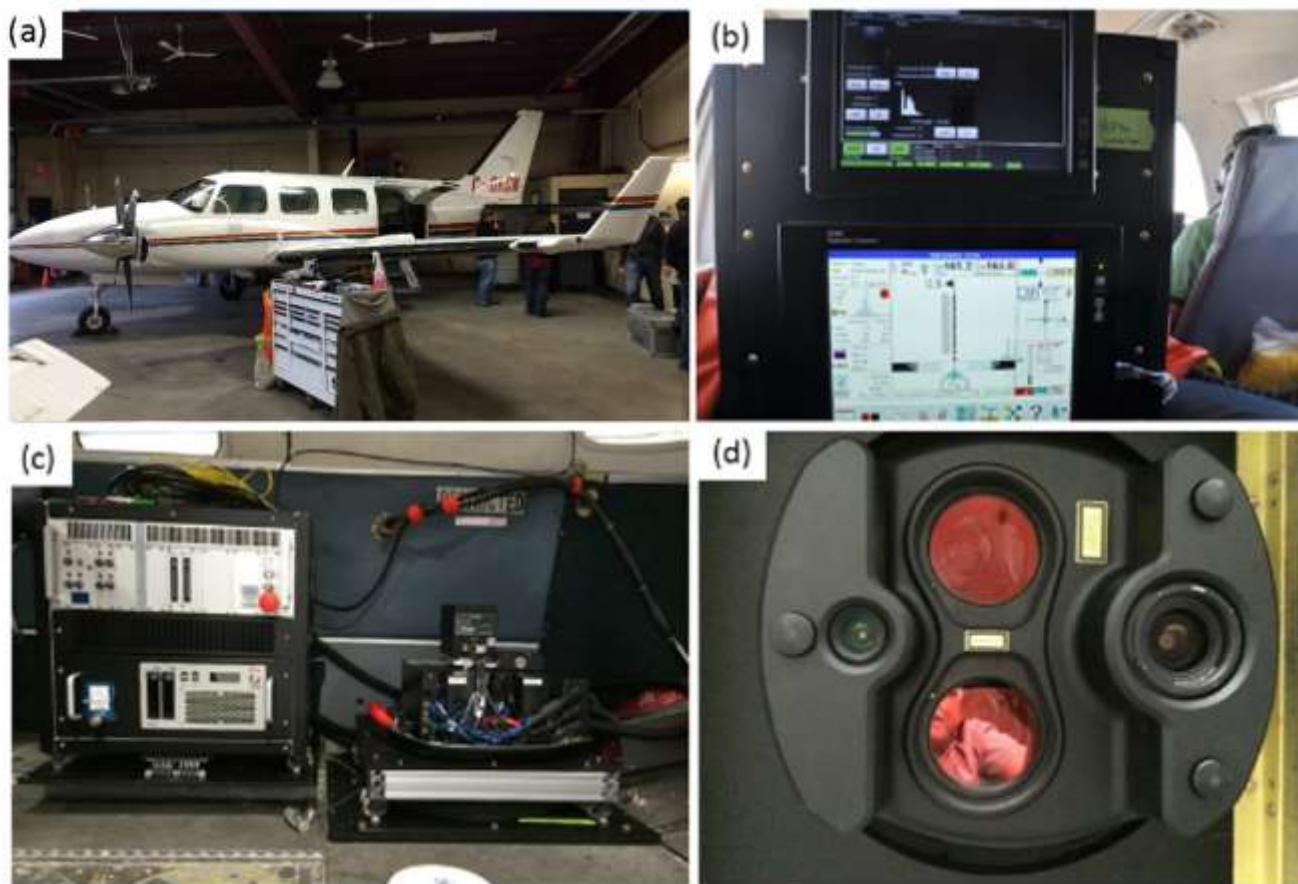


Figure 2.2: (a) Aircraft used for 2015 lidar survey; (b) display seen by lidar operator in-flight; (c) main body of sensor (right) and the data rack(left); (d) large red circles are the lasers; the RCD30 lens (right) and low resolution camera quality control(left).

2.2 Lidar Survey Details

The lidar surveys were conducted in October and November, 2015 (Table 1). The surveys were planned using Mission Pro software and flown at an altitude of 400 m above ground at a flying speed of 62 m/s. The planned flight lines for each study area are shown in Figure 2.3. The aircraft required ground-based high precision GPS data to be collected during the lidar survey in order to provide accurate positional data for the aircraft trajectory. Our Leica GS14 RTK GPS system was used to set up a base station over a known monument (typically a New Brunswick High Precision Network (HPN) or a Canadian Hydrographic Service Benchmark). The GPS base station was set to log observations at 1 second intervals and the RTK rover was used to collect lidar validation points on hard flat surfaces (Figure 2.3).

Study Area	Survey Date	Survey Time (UTC)
Saint-Simon Bay, NB	October 24, 2015	14:00 – 18:00
Tabusintac Bay North, NB	October 26, 2015	12:30 – 15:00
Tabusintac Bay North, NB	November 10, 2015	16:00 – 17:30
Cocagne River, NB	October 22, 2015	16:00 – 18:30

Table 1: 2015 lidar survey dates.

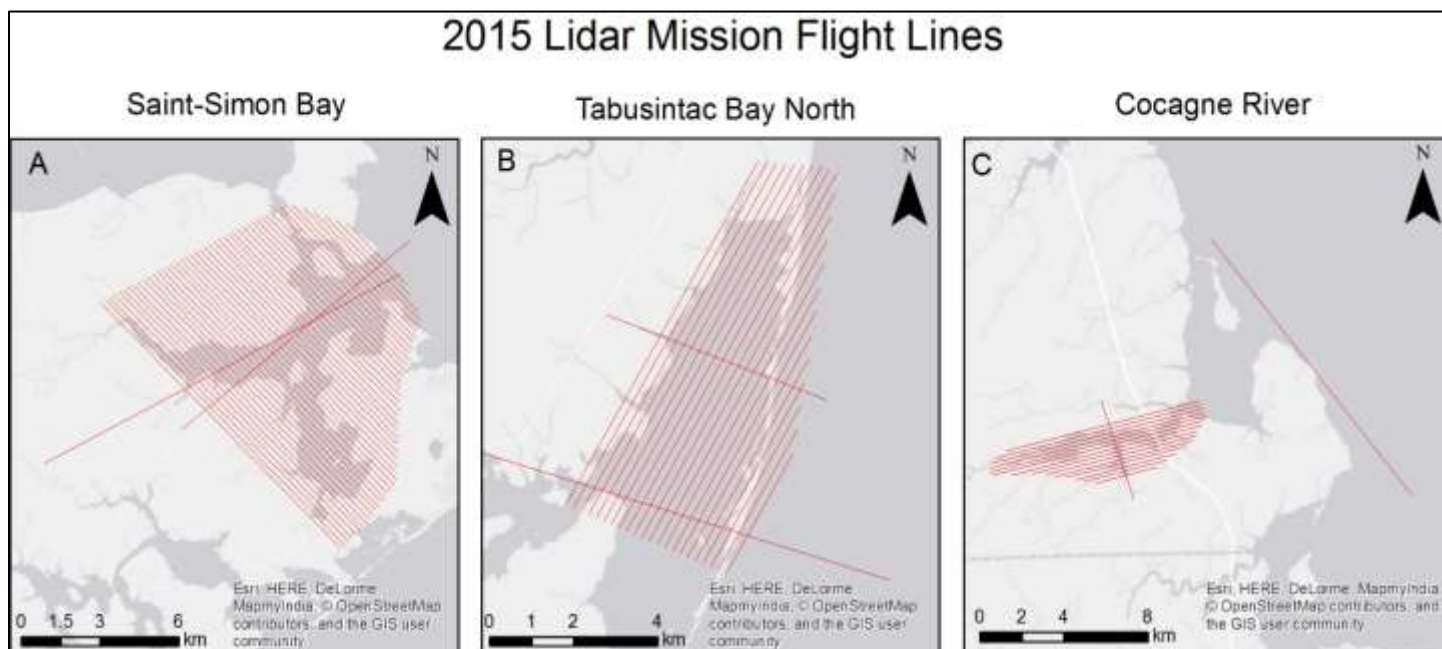


Figure 2.3: Flight lines planned for the 2015 study areas (A) Saint-Simon Bay, (B) Tabusintac Bay North, and (C) Cocagne River.

2.3 Ground Truth Data Collection

Ground truth data collection is an important aspect of topo-bathymetric lidar data collection. In 2015 we conducted our traditional “time-of-flight” ground truth data including hard surface validation and depth measurements to validate the lidar, Secchi depth measurements for information on water clarity, and underwater photographs to obtain information on bottom type and vegetation (Table 2, Figure 2.4). For the 2015 field season, we employed a new system to measure the seabed elevation directly using a large pole onto which we threaded the RTK GPS. This system helped to overcome the challenges of validating 1 m resolution lidar bathymetry using 3-5 m resolution code-based GPS to obtain the boat-based bathymetry spatial information. By threading the RTK GPS antenna on the pole and measuring the elevation of the seabed directly we not only benefitted from the higher resolution spatial data of the RTK GPS (2-5 cm accuracy), we also eliminated errors introduced into depth measurements obtained from a boat such as those caused by wave action, tidal variation, and angle of rope for lead ball drop measurements (Figure 2.4c). Table 2 summarizes the ground truth measurements undertaken for the three DFO PARR study areas in 2015, and Figure 2.5 shows a map of the distribution of ground truth measurements. Base stations are shown on Figure 1.1.

Topo-Bathymetric Lidar and Photographic Survey of Various Bays located in NB, NS, and PEI

Location	Date	Base station	GPS System	Secchi	Depth	Light Sensors	Underwater Photos	Hard Surface GPS
Saint-Simon	9-Oct-15	HPN 4674	GS14	Y	P, M, ES	Deployed	P	Y
	24-Oct-15*	HPN 4674	GS14	Y	P, M, ES	-	P, Q ₅₀ , SV	-
	11-Nov-15	HPN 4674	GS14	-	P	Retrieved	-	-
Tabusintac	7-Oct-15	Tabu_Wharf	GS14	Y	P,M, ES	Deployed	P, SV	-
	26-Oct-15*	Tabu_Wharf	GS14	Y	P, M, ES	Retrieved	P, Q ₅₀	Y
	10-Nov-15*	Tabu_Wharf	GS14	Y	P, M	-	P,Q ₅₀	-
Cocagne	8-Oct-15	HPN 8650	530	Y	DM, M	N/A	Q ₅₀	Y
	22-Oct-15*	HPN 8650	GS14	Y	P, DM, M	N/A	P,Q ₅₀	-

Table 2: Ground truth data summary. * Indicates that the ground truth survey was occurring simultaneously with the lidar survey. GPS Column: Two Leica GPS systems were used the GS14 and the 530. Depth Column: P=GPS antenna threaded onto the large pole for direct bottom elevation measurement; M=manual depth measurement using lead ball or weighted Secchi disk; DM=handheld single beam DepthMate echo sounder; ES=Single beam commercial grade Humminbird Echo Sounder. Underwater Photos: P=GoPro camera secured to pole for underwater still photos; Q₅₀=0.25 m² quadrat with downward-looking GoPro camera; SV=SeaViewer underwater video camera.

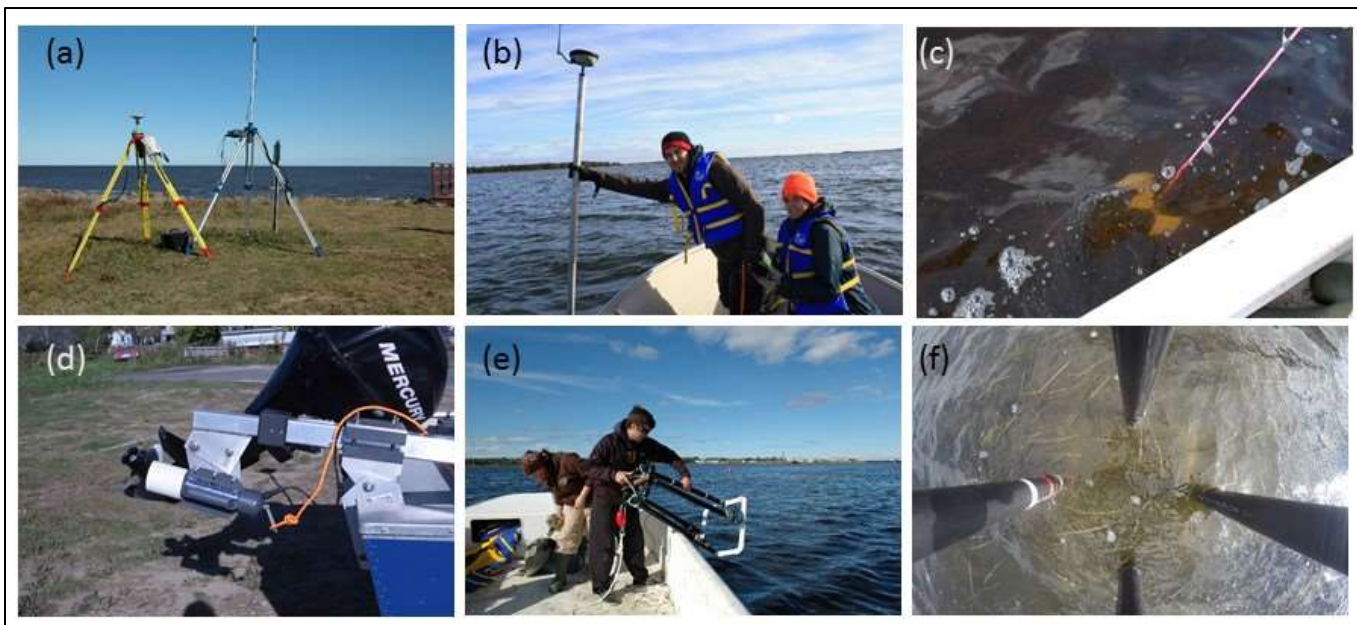


Figure 2.4: Ground truth images (a) GPS base station set up over HPN monument at Cocagne; (b) RTK GPS depth measurement using pole; (c) submerged Secchi disk; (d) Seaviewer underwater video camera; (e) 0.25 m² quadrat being deployed; (f) eelgrass at Tabusintac as photographed using quadrat.

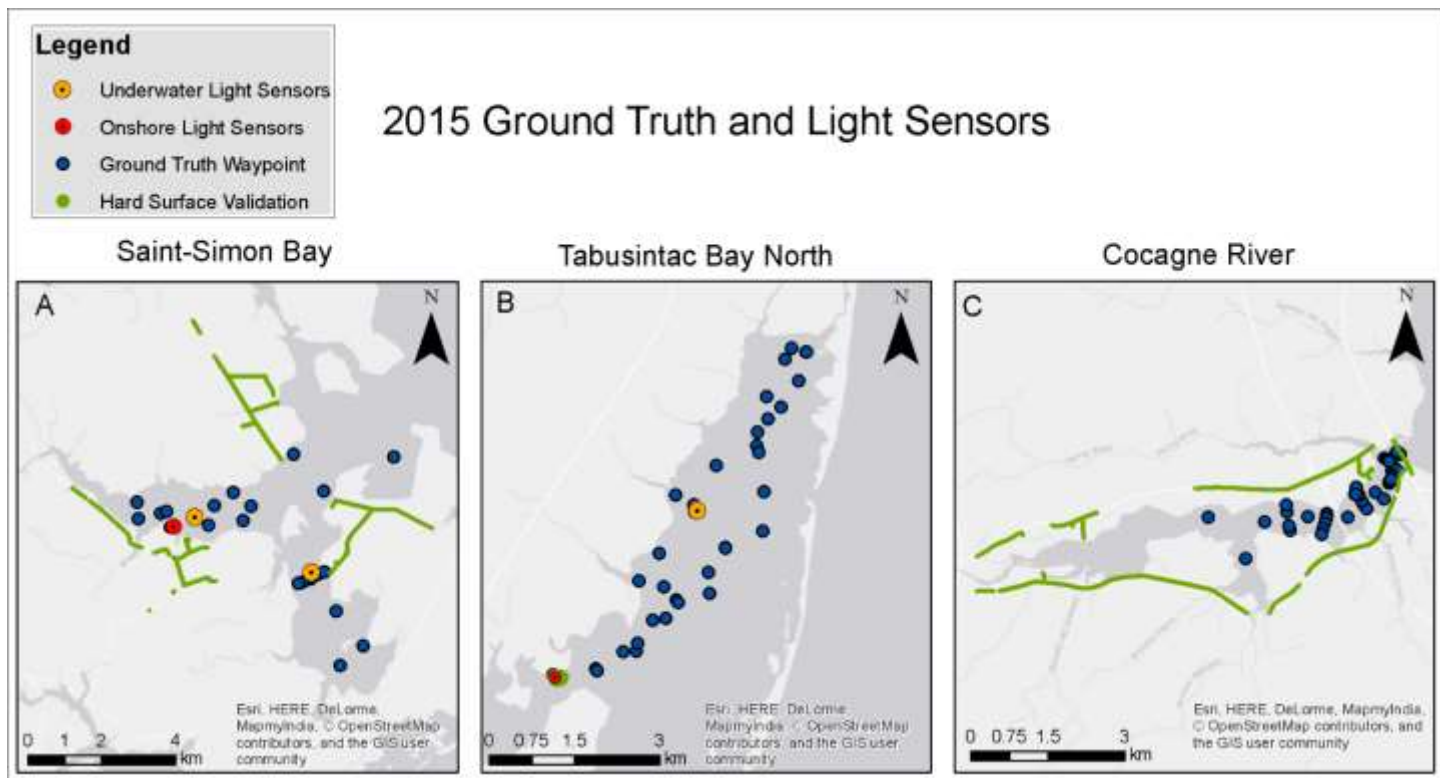


Figure 2.5: Location of hard surface GPS validation points, underwater and onshore light sensors, and boat-based ground truth waypoints at (A) Saint-Simon, (B) Tabusintac, and (C) Cocagne River. Note that no light sensors were deployed in Cocagne River, and there were no roads in the Tabusintac North study area for hard surface validation.

2.3.1 Light Sensors

The 2015 ground truth campaign also included the deployment of underwater light sensors. The sensors were Onset HOBO Light and Temperature Pendant Sensors, which are wireless monitoring devices that can be deployed remotely for months at a time and will log data at user selected intervals. For this study, two of the Hobo sensors were secured to a cinder block (Figure 2.6) and deployed at two locations in Saint-Simon, and at one location in Tabusintac (Figure 2.5), approximately one month prior to the lidar surveys (Table 2). The RTK pole was used to store the location of the sensor deployment, and a rope was attached to a second block which was deployed nearby, so that the equipment could be retrieved by dragging the anchor or grapple between the two GPS points. The Saint-Simon northern light sensors and the Tabusintac sensors were retrieved following the lidar surveys, but field crews were unable to locate the Saint-Simon southern sensors (Figure 2.5).

The Hobo light sensors measure ambient light rather than a specific bandwidth of light that is available for biology, but they are inexpensive and provide data for research on how water clarity in each study area responded to physical forcing such as wind speed and direction. The light sensor data are presented in Section 2.4.3.

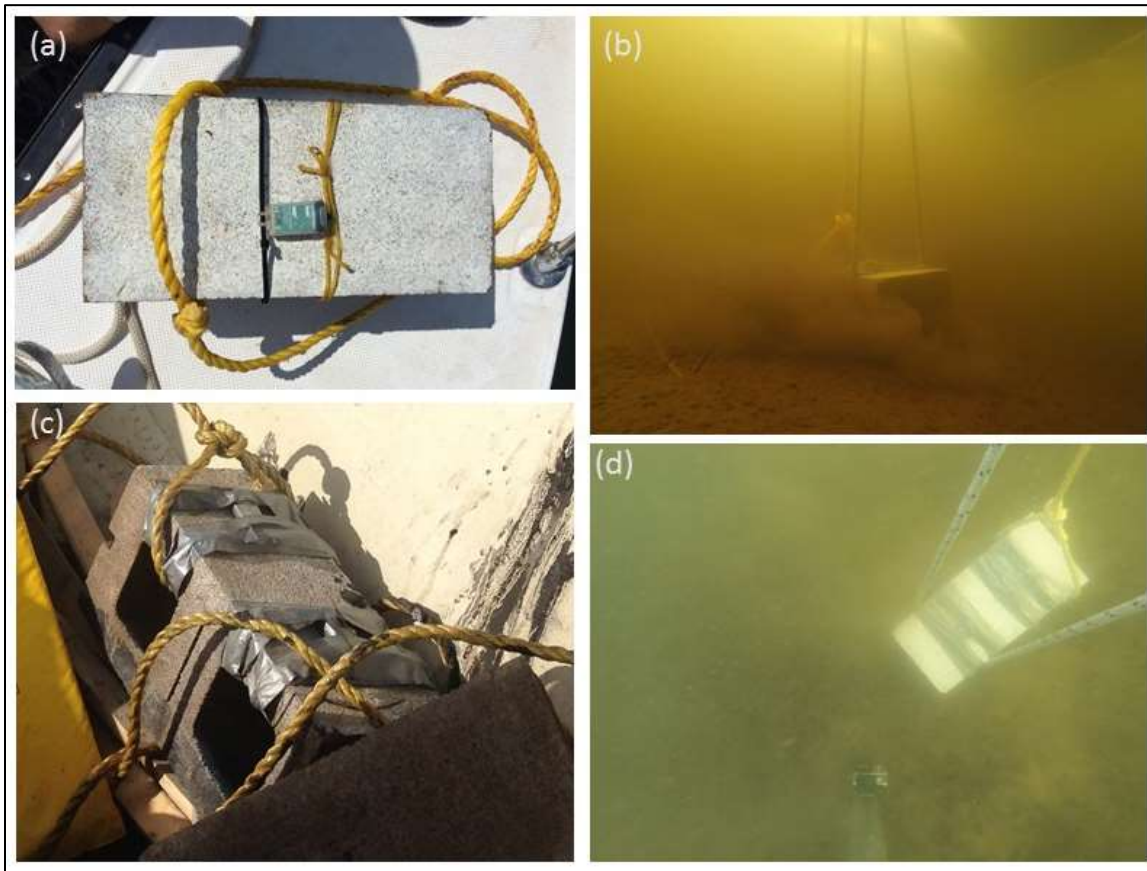


Figure 2.6: (a) A single light sensor secured to a cinder block (not used in PARR study areas); (b,d) underwater photo of cinder block and light sensor deployment at Tabusintac (b) and Saint Simon (d); (c) the light sensors after being retrieved from Tabusintac Bay in October.

2.3.2 Vegetation Ground Truth

Figure 2.7-Figure 2.10 show the locations of the underwater photographs conducted at Saint Simon, Tabusintac and Cocagne. The photos were used to assign each photo a value for percent eelgrass cover, based on the SeaGrassNet guidelines (<http://www.seagrassnet.org/>). Additionally, a qualitative visual inspection of the photos was completed to assign a water quality metric to each photograph, where 0 was indicative of water with very low clarity, 0.5 indicated medium clarity, or somewhat clear, and a rating of 1 indicated the water at that location at the time of the photograph was very clear. An eelgrass percent cover value of N/A indicates that water quality was too poor to detect any eelgrass.

The 2550 Series Offshore Fast Trolling colour video camera from SeaViewer Underwater Video Systems was used in Tabusintac for additional vegetation cover ground truth data collection. The video was streamed to a laptop in the boat and recorded using Pinnacle Studio. GPS information from a Garmin handheld receiver was included in the video stream via the Sea-Trak GPS Video Overlay system, also from SeaViewer. Eelgrass percent cover and water clarity metrics were derived in the same way as for the underwater still photographs.

Topo-Bathymetric Lidar and Photographic Survey of Various Bays located in NB, NS, and PEI

At Saint-Simon, eelgrass percent cover was 0 in two locations, and ranged between 25% and 80% in the other 16 locations (Figure 2.7). Water clarity was generally somewhat clear or clear; only four locations were classified as 0, or not clear. At Tabusintac, eelgrass was only detected in one location on Oct. 26; poor water quality obscured the bottom and no classification of eelgrass was possible (Figure 2.8a). On Nov. 10, eelgrass percent cover ranged from 5-55% and was detected only on the eastern side of the bay, and water clarity remained poor on the western side of the bay (Figure 2.8b). The underwater video imagery indicated eelgrass percent cover between 0% near the channel and up to 30% near the center of the bay (Figure 2.9). At Cocagne eelgrass percent cover ranged from 0% in the channel to 95% elsewhere and water clarity ranged between poor and moderate quality (Figure 2.10).

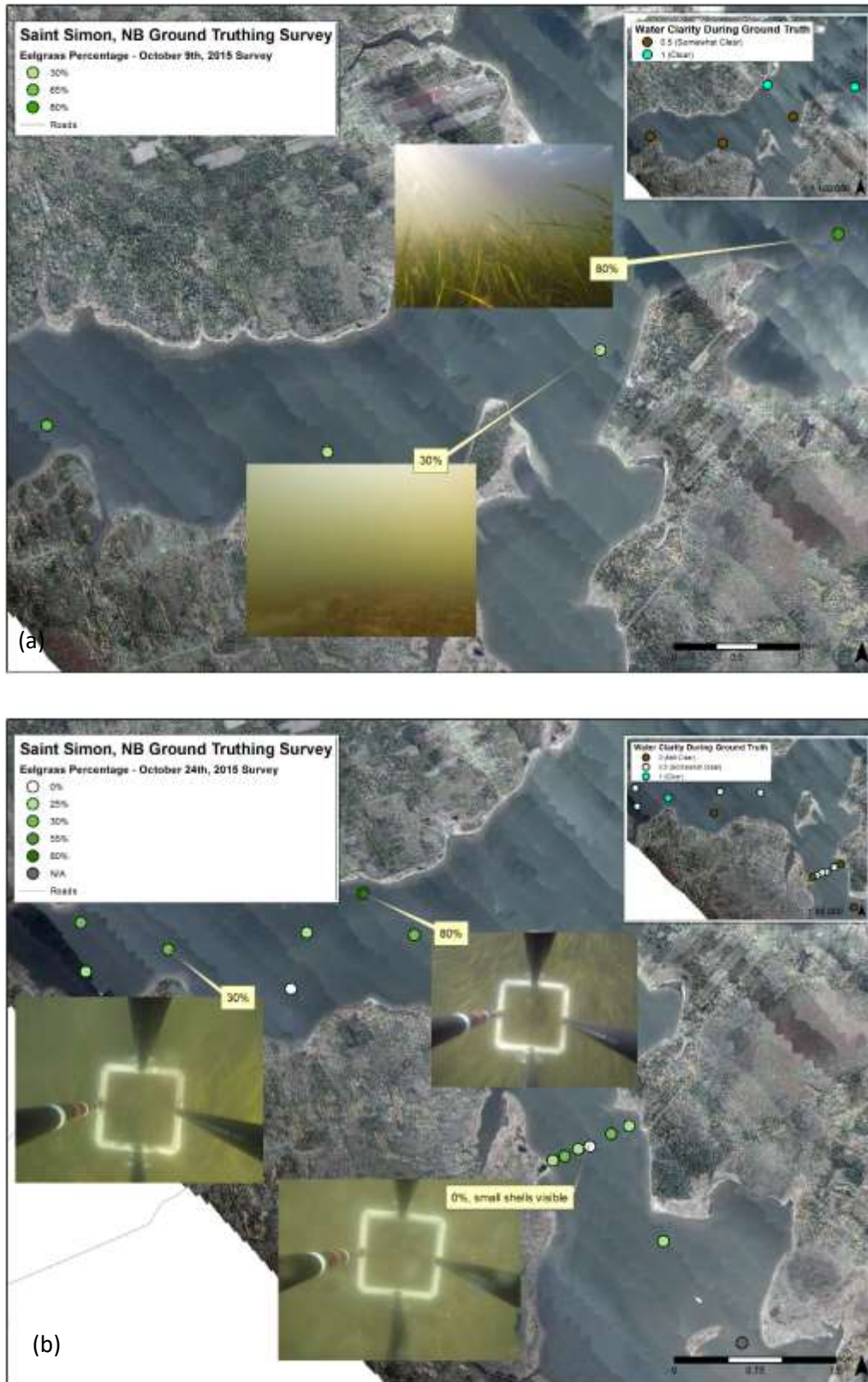


Figure 2.7: Saint Simon underwater photo ground truth on (a) October 9 and (b) October 24. N/A indicates no underwater photograph was taken, or the visibility was too poor to assess eelgrass presence. Background image is RCD30 orthophoto RGB mosaic.

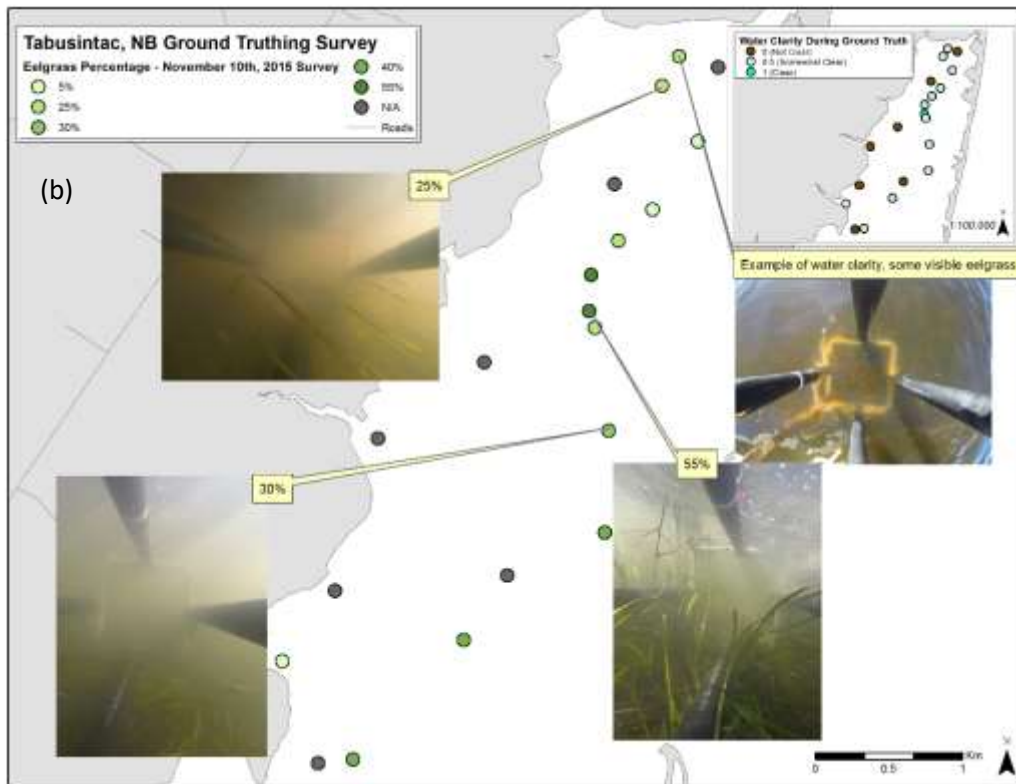
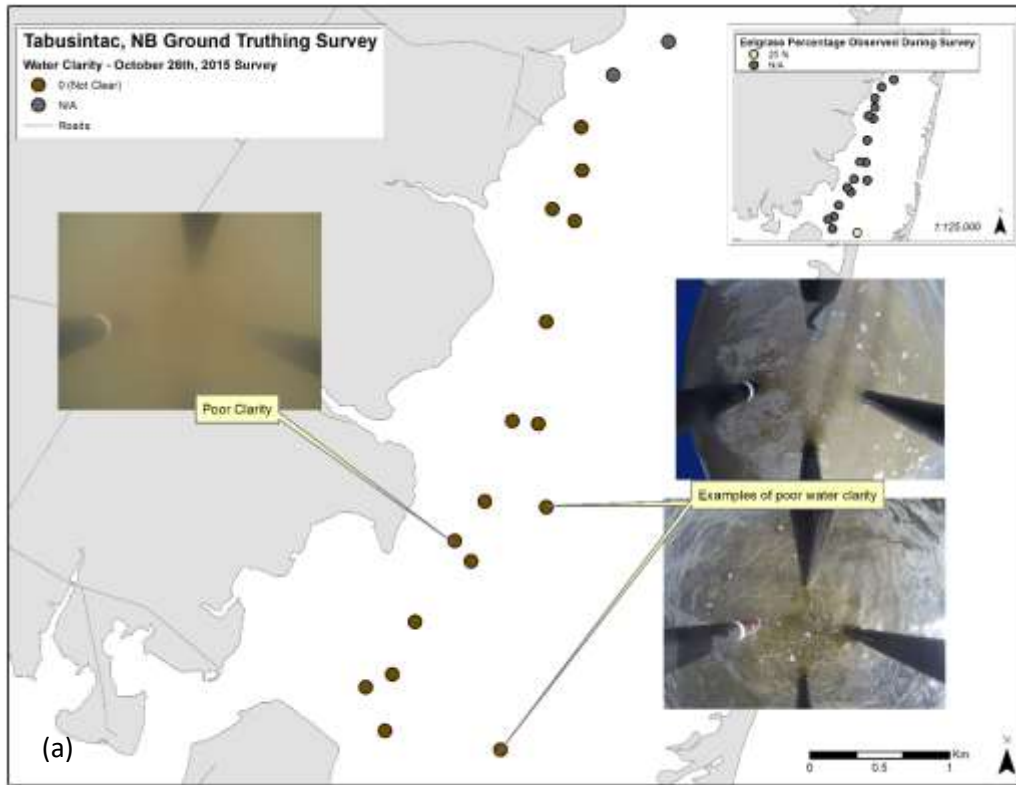


Figure 2.8: Tabusintac underwater photo ground truth on (a) October 26 and (b) November 10. N/A indicates no underwater photograph was taken, or the visibility was too poor to assess eelgrass presence.

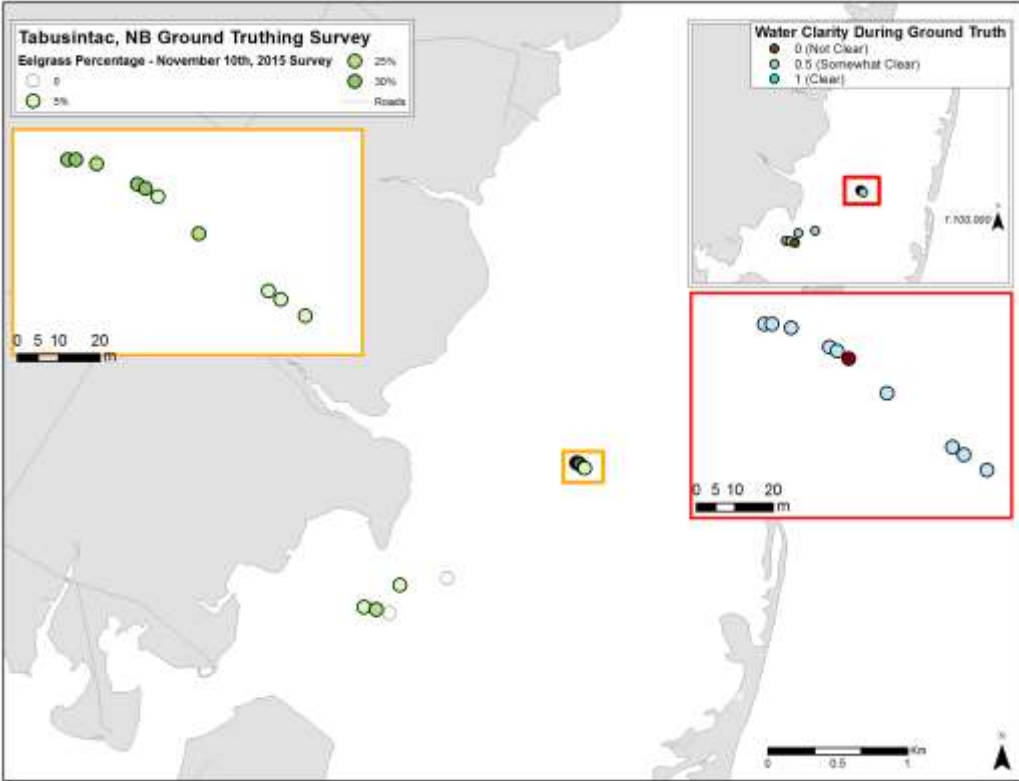


Figure 2.9: Tabusintac underwater video ground truth on October 7. Orange and red boxes are zoomed in on the transect at the center of the bay to show eelgrass (orange box) and water quality (red box).

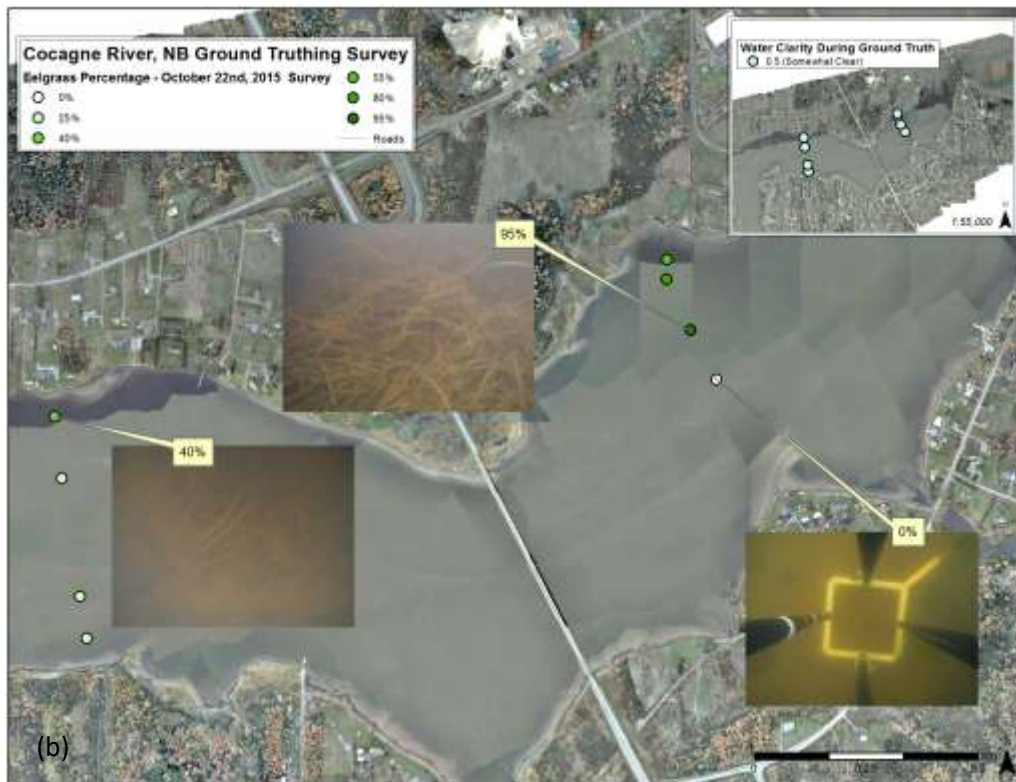
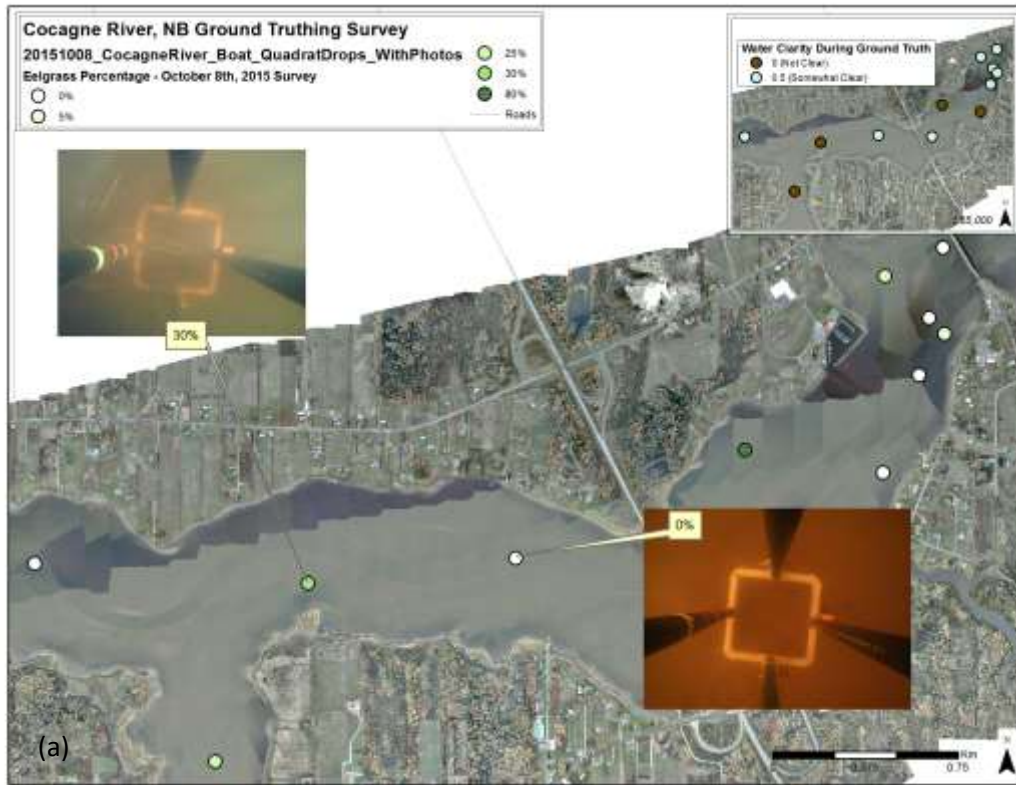


Figure 2.10: Cocagne River underwater photo ground truth on (a) October 8 and (b) October 22. N/A indicates no underwater photograph was taken, or the visibility was too poor to assess eelgrass presence. Background image is RCD30 orthophoto RGB mosaic.

2.4 Meteorological, Light and Tidal Conditions

2.4.1 Meteorology

Meteorological conditions during and prior to topo-bathy lidar data collection are an important factor in successful data collection. As the lidar sensor is limited by water clarity, windy weather has the potential to stir up any fine sediment in the water and prevent good laser penetration. Rainy weather is not suitable for lidar collection, and the glare of the sun must also be factored in for the collection of aerial photography. Before each lidar survey we monitored weather forecasts using a variety of forecasting websites (www.intellicast.com, www.windfinder.com, <http://weather.gc.ca/marine/>, <http://weather.gc.ca/>) as well as current and past conditions using the closest EC weather station to the study sites. For Saint-Simon the nearest EC weather station was Bas Caraquet, the EC Miramichi station was used for Cocagne, and as Tabusintac is located between these two stations we typically monitored both for a better representation of weather at Tabusintac (Figure 1.1).

The wind during the lidar survey at Saint-Simon was suitable for good data collection. The wind was low at the onset of the survey, and picked up to near 10 km/h towards the end of the survey, blowing from the south (Figure 2.11, blue box). There were several days in the week preceding the survey when 30 km/hr wind from the northwest made surveying unsuitable, but particulate matter stirred up from these events settled quickly. Cocagne River was surveyed on Oct. 22 during a period of low wind (<10 km/hr) blowing from the south (Figure 2.12, yellow box). Wind events of 35 km/hr and 25 km/hr occurred on October 20 and 21, respectively, both blowing from the northwest, but the ground crew found that any wind-induced turbidity had resolved by the time of the survey.

On October 26 at Tabusintac the wind at Miramichi was blowing from the northwest at nearly 20 km/hr (Figure 2.12, red box), and closer to 30 km/hr at Bas Caraquet (Figure 2.11, red box). It was expected that the study area, being in the northern section of Tabusintac Bay, would be sheltered somewhat from a northwest wind, which was forecast to be a lighter wind, and so the survey was completed. However, the sediment stirred up by the wind presented challenges for both the ground crew and the lidar data products. Figure 2.13a-c show the choppy water surface and poor water clarity on October 26. Upon review of the data after survey completion, it was decided that a second attempt would be made to survey Tabusintac. Operational and logistical challenges prevented survey activity during the calm weather in the first week of November, the survey was attempted for a second time on November 10. Wind conditions were similar at Bas Caraquet and Miramichi during the survey, blowing at ~20 km/hr from the northwest and changing to an eastern wind during the survey. Figure 2.13d shows the improvement in conditions during the second survey, despite the similarities in the wind speeds recorded during the two surveys. Unfortunately, the flight was aborted when it was two thirds completed due to a problem with the lidar system. Overcoming these challenges to lidar operational efficiency related to weather forecasts and publicly available observations is an active area of research at AGRG and is funded through an NSERC Applied Research and Development grant.

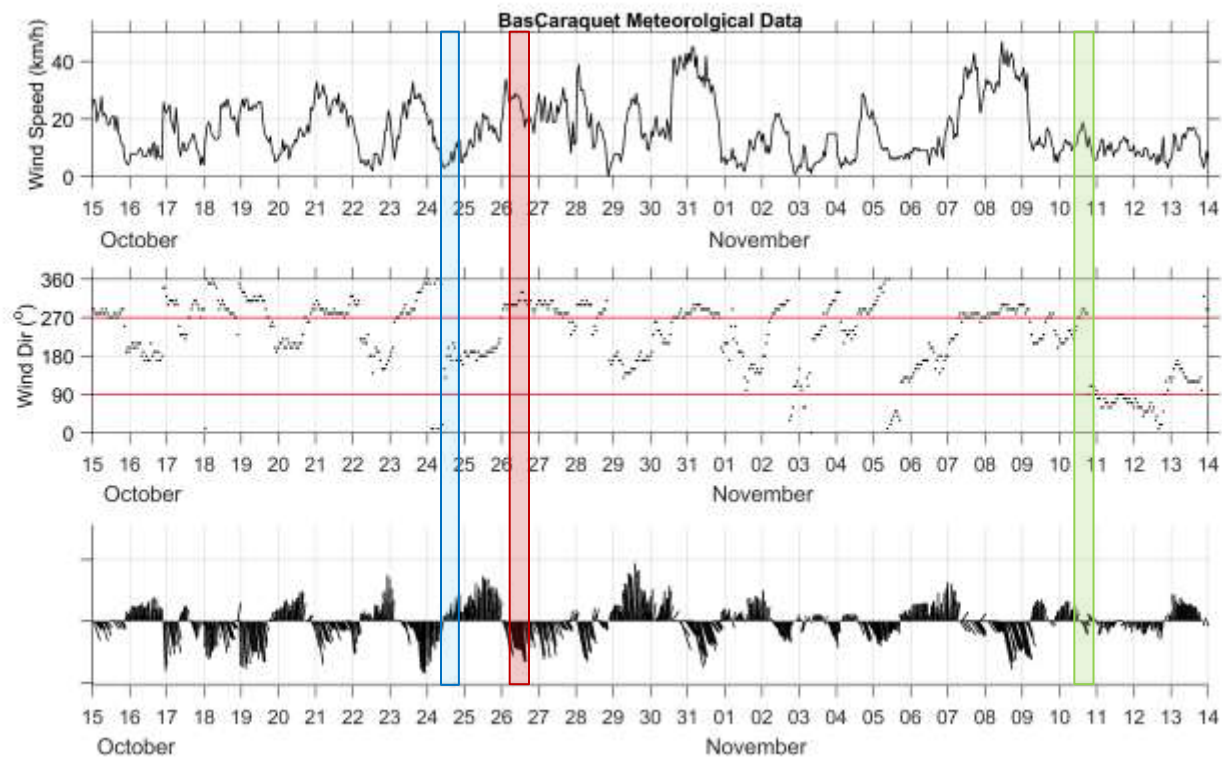


Figure 2.11: Wind speed (top panel) and direction (middle panel) collected at the EC weather station at Bas Caraquet between October 15 and November 14, 2015 at 1 hour intervals. The lower panel shows a stick plot of the wind, where the sticks point in the direction the wind is blowing, and the boxes indicates the lidar surveys (blue = Saint-Simon, red = Tabusintac Survey 1, green = Tabusintac Survey 2).

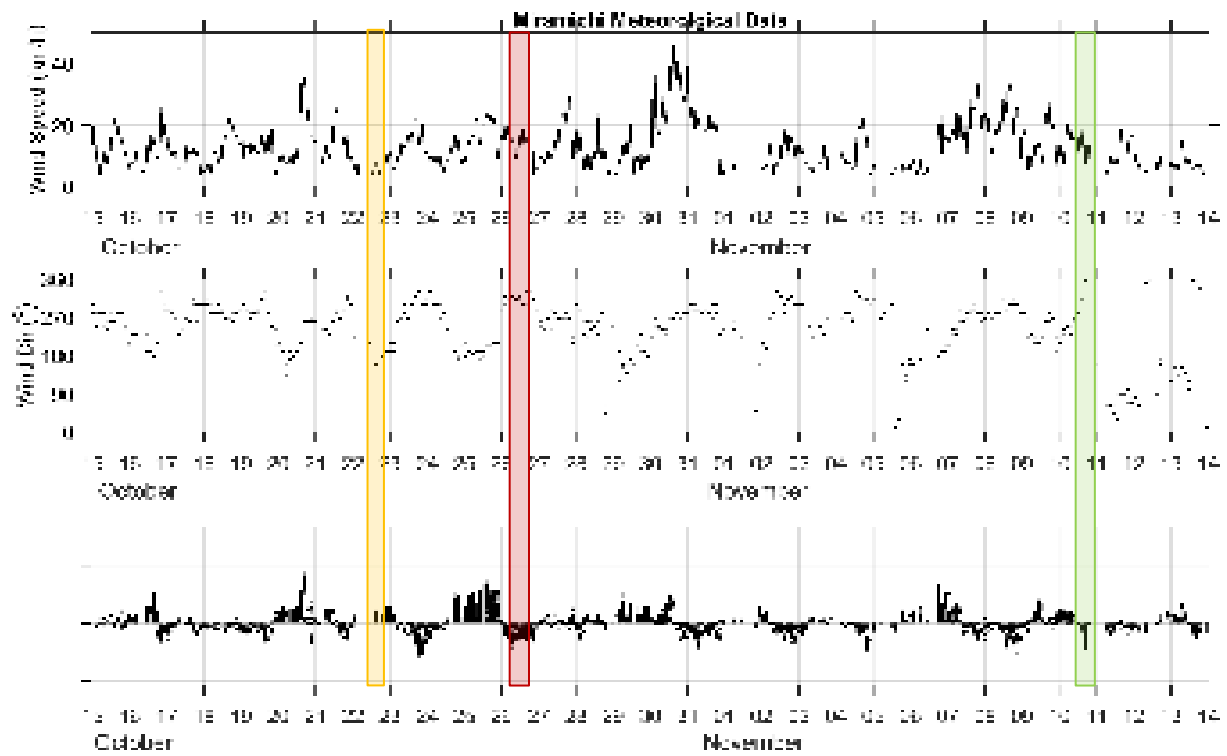


Figure 2.12: Wind speed (top panel) and direction (middle panel) collected at the EC weather station at Miramichi, NB between October 15 and November 14, 2015 at 1 hour intervals. The lower panel shows a stick plot of the wind, where the sticks point in the direction the wind is blowing, and the boxes indicates the lidar surveys (orange = Cocagne, red = Tabusintac Survey 1, green = Tabusintac Survey 2).

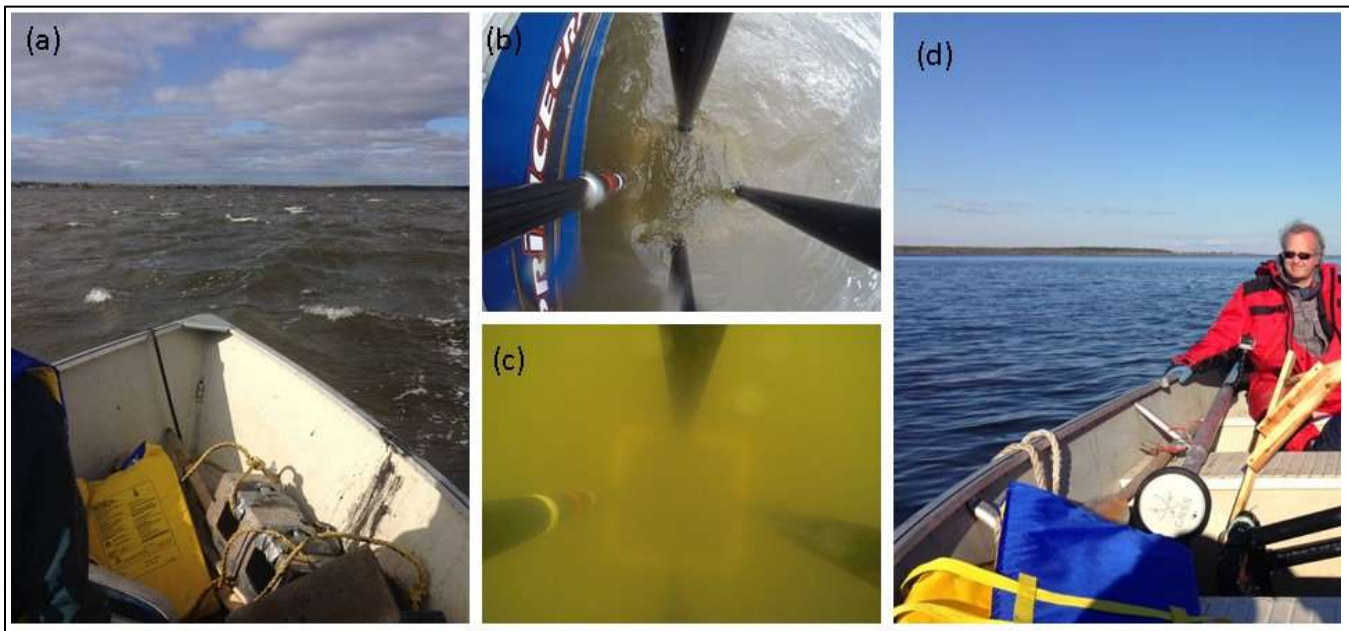


Figure 2.13: (a,b,c) Conditions at Tabusintac on October 26, where wind caused rough seas and reduced water clarity. (d) shows improved conditions on November 10 during the second survey.

2.4.2 Tide

Optimal data collection is a balance not only of water clarity and meteorological conditions, but also of daylight and tidal stage. The surveys were completed as near to low tide as weather and daylight permitted in order to reduce the amount of water that the laser was required to penetrate through in order to reach the seabed (Figure 2.14). On November 10 (Figure 2.14c) the second Tabusintac survey was delayed as long as possible as the forecast indicated lowest winds near the late afternoon, and the decision was made to optimize for low wind rather than low tide. At Cocagne (Figure 2.14d), the lowest tide was missed as the aircraft waited out some rain showers that were interfering with good lidar collection. Transit times to each study area from the base of operations in Fredericton played a role in when an area was surveyed, as well as time on the ground to refuel for larger areas (e.g., Saint-Simon).

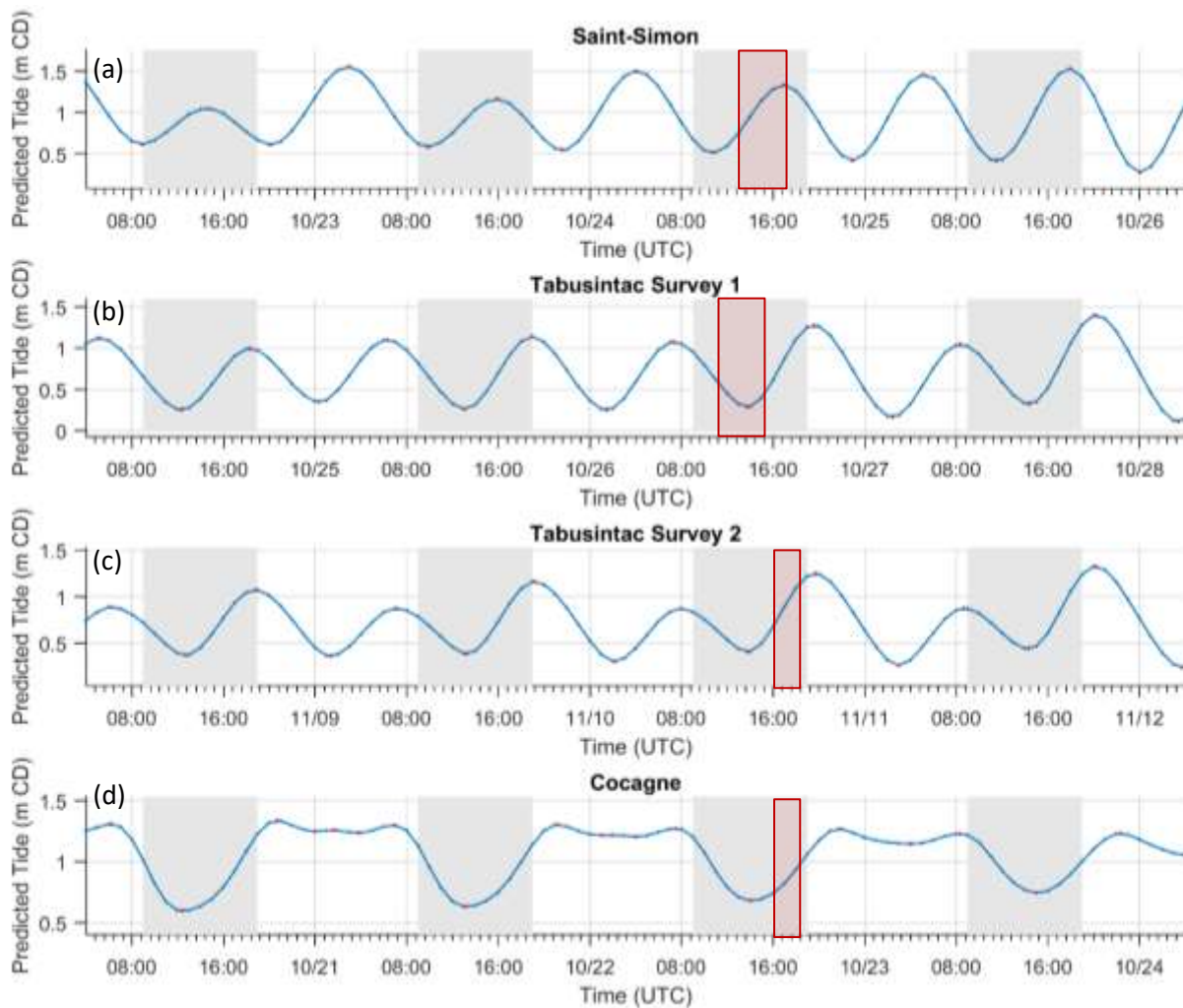


Figure 2.14: Tides for surveys at (a) Saint-Simon; (b) Tabusintac Survey 1; (c) Tabusintac Survey 2; (d) Cocagne. Grey bars indicate daylight hours and red boxes indicate survey durations.

2.4.3 Light

The light sensor measures ambient light in units of Lux (lumens m⁻²). The sensors were calibrated prior to deployment by mounting all sensors in direct sunlight for 250 minutes and grouping them based on similar readings after the calibration trial. The percent of underwater light was calculated to remove the effects of variations in cloud cover using the following equation:

$$\% UW \text{ light} = 100 \times \frac{UW \text{ light}}{OS \text{ light}}$$

where UW = underwater and OS=onshore. Figure 2.15 shows the variations in light due to water clarity and tide at Saint-Simon and Tabusintac; note the difference in y-axis at each study site. At Saint Simon, the sensors were deployed in approximately 3 m of water near low tide, and typically less than 5% of sunlight available at the surface reached the sensors. At Tabusintac the sensors were deployed in approximately 1 m of water at low tide and typically about 20% of light available at the surface reached the sensors.

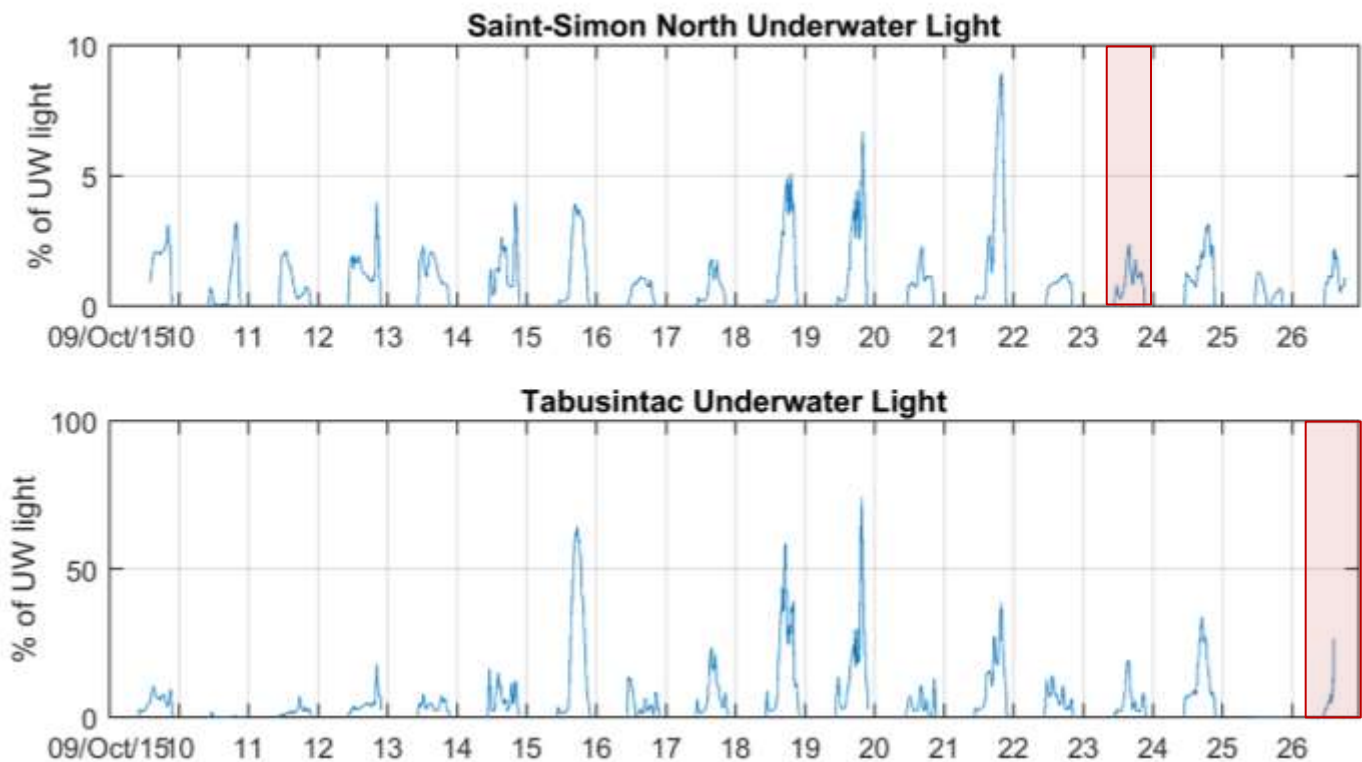


Figure 2.15: Light sensor data at (a) Saint-Simon North and (b) Tabusintac. The % of underwater light is underwater light divided by onshore light. Red boxes indicate lidar survey dates. The blue lines are an average of the two sensors which were placed on each cinder block.

2.5 Elevation Data Processing

2.5.1 Lidar processing

2.5.1.1 Point Cloud Processing

Once the GPS trajectory was processed for the aircraft utilizing the GPS base station and aircraft GPS observations were combined with the inertial measurement unit, the navigation data was linked to the laser returns and georeferenced. Lidar Survey Studio (LSS) software accompanies the Chiroptera II sensor and is used to process the lidar waveforms into discrete points. The data can then be inspected to ensure there was sufficient overlap (30%) and no gaps exist in the lidar coverage.

One critical step in the processing of bathymetric lidar is the ability to map the water surface. This is critical for two components of georeferencing the final target or targets that the reflected laser pulse recorded: the refraction of the light when it passes from the medium of air to water and the change in the speed of light from air to water. The LSS software computes the water surface from the lidar returns of both the topo and bathy lasers. In addition to classifying points as land, water surface or bathymetry, the system also computes a water surface that ensures the entire area of water surface is covered regardless of the original lidar point density. As mentioned, part of the processing involves converting the raw waveform lidar return time series into discrete classified points using LSS signal processing; points include ground, water surface, seabed, etc. Waveform processing may include algorithms specifically for classifying the seabed. The points were examined in LSS both in plan view and in cross-section view. The waveforms can be queried for each point so that the location of the waveform peak can be identified and the type of point defined, for example water surface and bathymetry.

The LAS files were read into TerraScan™ with the laser returns grouped by laser type so they could be easily separated, analyzed and further refined. Because of the differences in the lidar footprint between the topo and bathy lasers, the bathy point returns would be used to represent the water surface and bathymetry points and the topo points would be used to represent targets on the land. See Table 3 and the attached Data Dictionary report for the classification codes for the delivered LAS 1.2 files. The refined classified LAS files were read into ArcGIS™ and a variety of raster surfaces at a 2 m spatial sampling interval were produced.

Table 3. Lidar point classification Codes and descriptions. Note that ‘overlap’ is determined for points which are within a desired footprint of points from a separate flight line; the latter of which having less absolute range to the laser sensor.

Class number	Description
0	Water model
1	Bathymetry (Bathy)
2	Bathy Vegetation
3	N/A
4	Topo laser Ground
5	Topo laser non-ground (vegetation & buildings)
6	Hydro laser Ground
7	Bathy laser non-ground
8	Water
9	Noise
10	Overlap Water Model
11	Overlap Bathy
12	Overlap Bathy Veg
13	N/A
14	Overlap Topo Laser Ground
15	Overlap Topo Laser Veg
16	Overlap Bathy Laser Ground
17	Overlap Bathy Laser Veg
18	Overlap Water
19	Overlap Noise

2.5.1.2 Gridded Surface Models

There are three main data products derived from the lidar point cloud. The first two are based on the elevation and include the Digital Surface Model (DSM) which incorporates valid lidar returns from vegetation, buildings, ground and bathymetry returns, and the Digital Elevation Model (DEM) which incorporates ground returns above and below the water line. The third data product is the intensity of the lidar returns, or the reflectance of the bathy laser. The lidar reflectance, or the amplitude of the returning signal from the bathy laser, is influenced by several factors including water depth, the local angle of incidence with the target, the natural reflectivity of the target material, the transmission power of the laser and the sensitivity of the receiver.

2.5.1.3 Depth Normalization of the Green Laser

The amplitude of the returning signal from the bathy laser provides a means of visualizing the seabed cover, and is influenced by several factors including water depth and clarity, the local angle of incidence with the target, the natural reflectivity of the target material, and the voltage or gain of the transmitted lidar pulse. The raw amplitude data are

Topo-Bathymetric Lidar and Photographic Survey of Various Bays located in NB, NS, and PEI

difficult to interpret because of variances as a result of signal loss due to the attenuation of the laser pulse through the water column at different scan angles. Gridding the amplitude value from the bathy laser results in an image with a wide range of values that are not compensated for depth and have significant differences for the same target depending on the local angle of incidence from flight line to flight line. As a result, these data are not usable as is for quantitative analysis and are difficult to interpret for qualitative analysis. We have designed a process to normalize the amplitude data for signal loss in a recent publication (Webster et al, 2016). The process involved sampling the amplitude data from a location with homogeneous seabed cover (e.g., sand or eelgrass) over a range of depths. These data were used to establish a relationship between depth and the logarithm of the amplitude value. The inverse of this relationship was used with the depth map to adjust the amplitude data so that they could be interpreted without the bias of depth. A depth normalized amplitude/intensity image (DNI) was created for each study site using this technique that can be more consistently interpreted for the seabed cover material. Note that this analysis considers only bathymetric lidar values and ignores any topographic elevation points.

2.5.1.4 Aerial Photo Processing

The RCD30 60 MPIX imagery was processed using the aircraft trajectory and direct georeferencing. The low altitude and high resolution of the imagery required that the lidar data be processed first to produce bare-earth digital elevation models (DEMs) that were used in the orthorectification process. The aircraft trajectory, which blends the GPS position and the IMU attitude information into a best estimate of the overall position and orientation of the aircraft during the survey. This trajectory, which is linked to the laser shots and photo events by GPS based time tags, is used to define the Exterior Orientation (EO) for each of the RCD30 aerial photos that were acquired. The EO, which has traditionally been calculated by selecting ground control point (x, y, and z) locations relative to the air photo frame and calculating a bundle adjustment, was calculated using direct georeferencing and exploiting the high precision of the navigation system. The EO file defines the camera position (x, y, z) for every exposure as well as the various rotation angles about the x, y and z axis known as omega, phi and kappa. The EO file along with a DEM was used with the aerial photo to produce a digital orthophoto. After the lidar data were processed and classified into ground points, the lidar-derived DEM (above and below the water line) was used in the orthorectification process in Erdas Imagine software and satisfactory results were produced.

2.5.2 Ellipsoidal to Orthometric Height Conversion

The original elevation of any lidar products are referenced to the same elevation model as the GPS they were collected with. This model is a theoretical Earth surface known as the ellipsoid, and elevations referenced to this surface are in ellipsoidal height (GRS80). To convert them to orthometric height (Oht), which is height relative to the Canadian Geodetic Vertical Datum of 1928 (CGVD28), an offset must be applied. The conversions are calculated based on the geoid-ellipsoid separation model, HT2, from Natural Resources Canada.

Topo-Bathymetric Lidar and Photographic Survey of Various Bays located in NB, NS, and PEI

Study Area	Conversion
Saint-Simon	Ellipsoid to CVGD28
Tabusintac	CHS Local Benchmark
Cocagne	Ellipsoid to CVGD28

2.6 Lidar Validation

Ground elevation measurements obtained using the RTK GPS system were used to validate the topographic lidar returns on areas of hard, flat surfaces. At Saint-Simon and Cocagne the GPS antenna was mounted on a vehicle and data were collected along roads within the study areas, while at Tabusintac points were collected along the only hard surface within the study area, the wharf (Figure 2.5).

Boat-based ground truth data were used to validate the bathymetric lidar returns (Figure 2.5). Although various methods were used to measure depth during fieldwork, only points measured using the large pole fitted with the RTK GPS antenna to directly measure the seabed were used for the accuracy assessment; points that measured depth using sonar or a weighted rope were not considered.

For both hard surface and boat-based GPS points, the differences in the GPS elevation and the lidar elevation (ΔZ) were calculated by extracting the lidar elevation from the DEM at the checkpoint and subtracting the lidar elevation from the GPS elevation. GPS points were subject to a quality control assessment such that the standard deviation of the elevation was required to be < 0.05 m.

3 Results

3.1 Lidar Validation

3.1.1 Topographic Validation

At Saint-Simon there were 3030 data points collected along the roads with a calculated mean ΔZ of $0.11 \text{ m} \pm 0.03 \text{ m}$; at Tabusintac there were 47 data points collected along the wharf and parking lot with a mean ΔZ of $0.20 \text{ m} \pm 0.07 \text{ m}$; at Cocagne there were 3154 data points collected along the roads, mean ΔZ was $0.05 \text{ m} \pm 0.03 \text{ m}$.

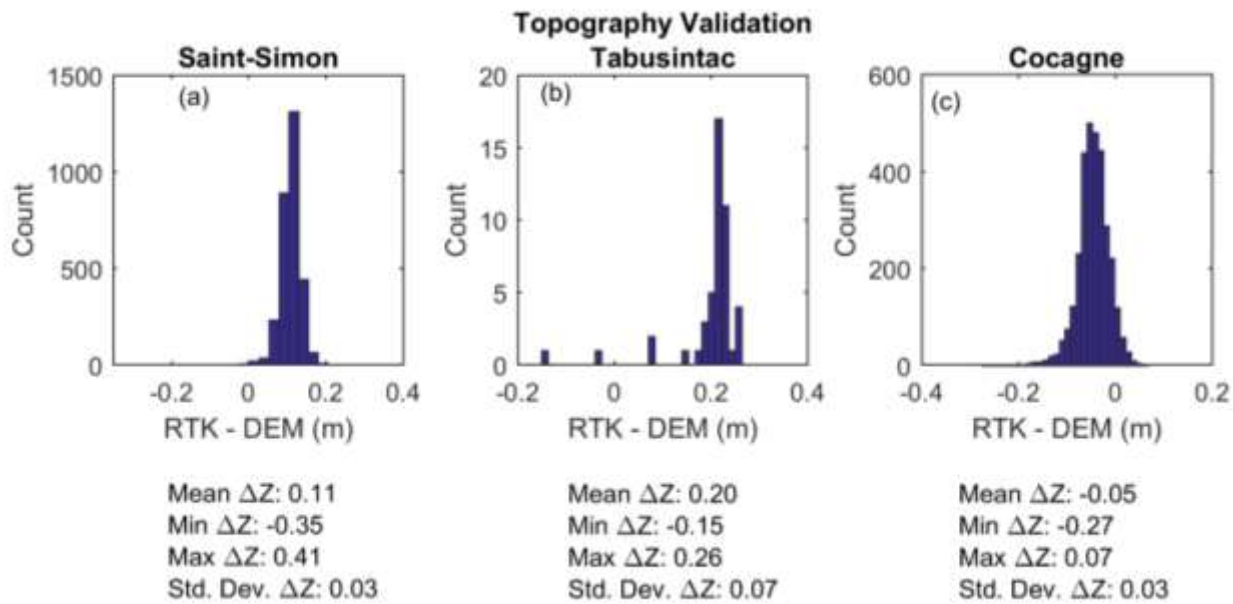


Figure 3.1: Topographic lidar validation for (a) Saint-Simon, (b) Tabusintac, and (c) Cocagne.

3.1.2 Bathymetric Validation

At all three study areas the mean ΔZ was negative, an indication that the DEM elevation is less (shallower) than the observed GPS point. At Saint-Simon, there were 21 GPS points, mean ΔZ was $-0.22 \text{ m} \pm 0.27 \text{ m}$; at Tabusintac there were 35 GPS points, mean ΔZ was $-0.23 \text{ m} \pm 0.22 \text{ m}$; at Cocagne there were 28 GPS points, mean ΔZ was $-0.27 \text{ m} \pm 0.18 \text{ m}$. It is possible that the bathymetric laser encountered difficulty in penetrating through the vegetation cover to the seabed, resulting in a derived seabed that is actually representative of the elevation of the eelgrass beds.

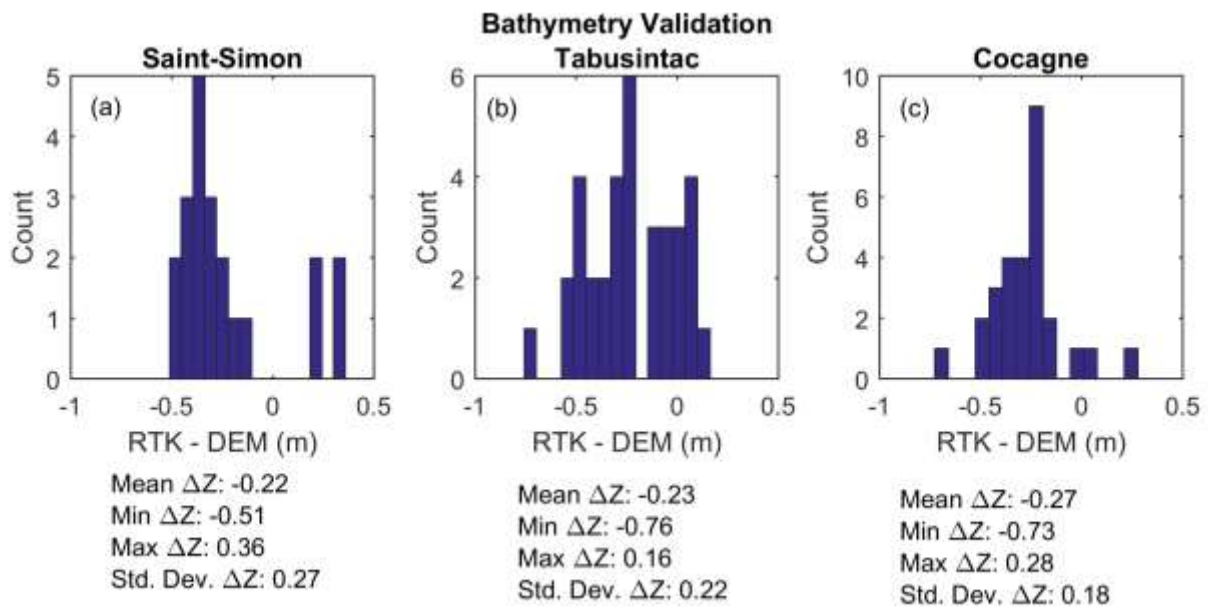


Figure 3.2: Bathymetric validation at (a) Saint-Simon; (b) Tabusintac; (c) Cocagne.

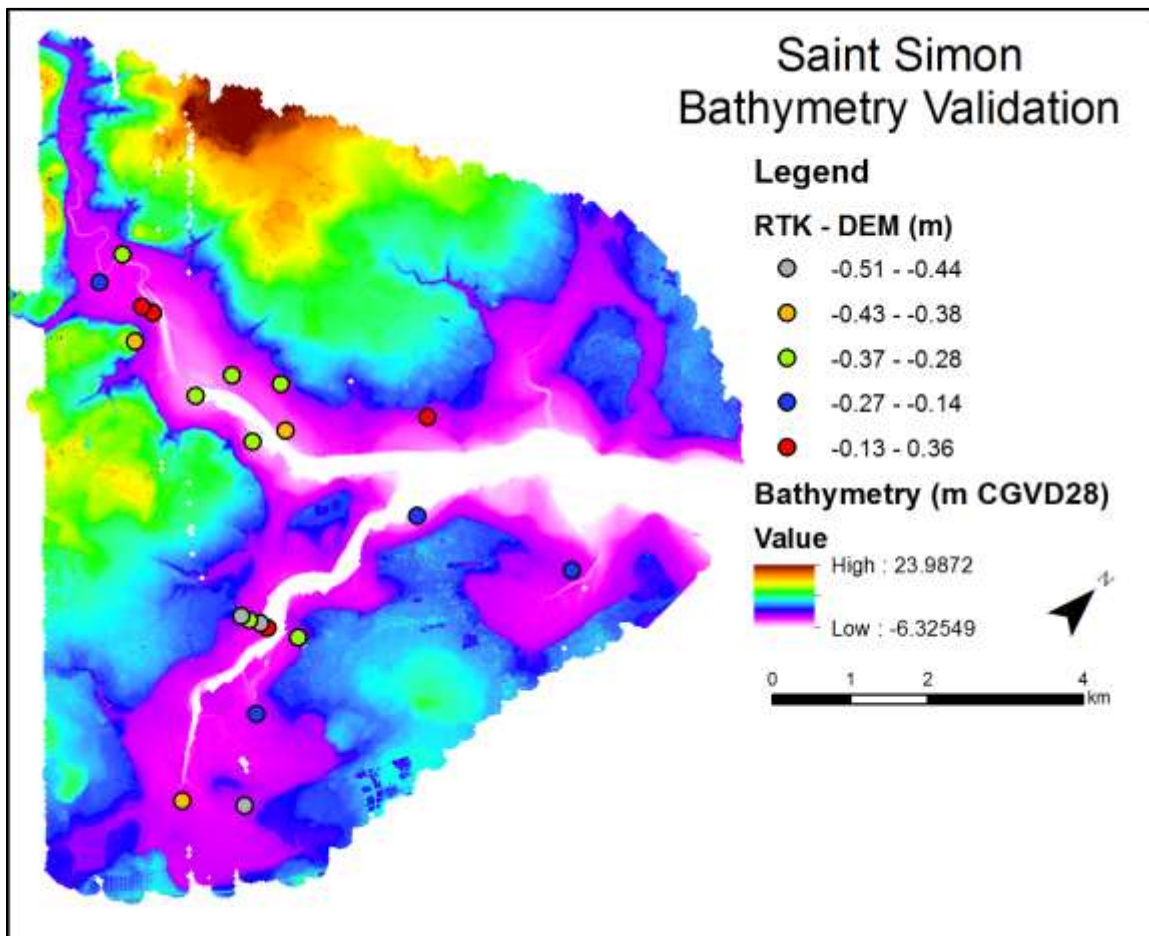


Figure 3.3: Saint Simon Bathymetry validation.

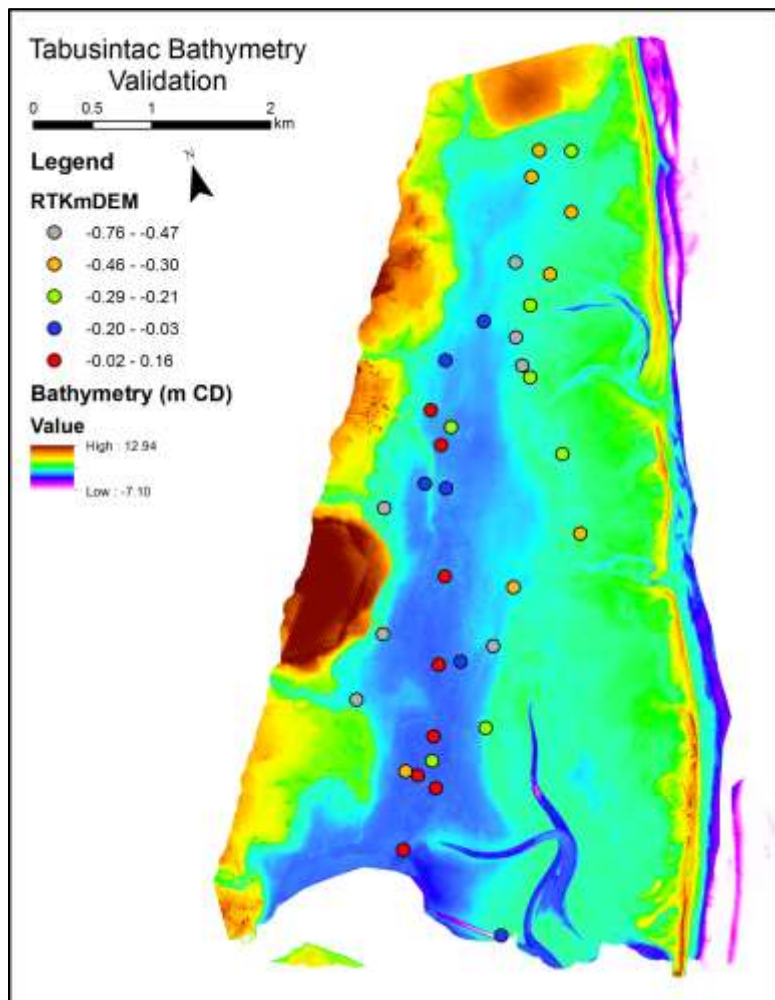


Figure 3.4: Tabusintac Bathymetric Validation.

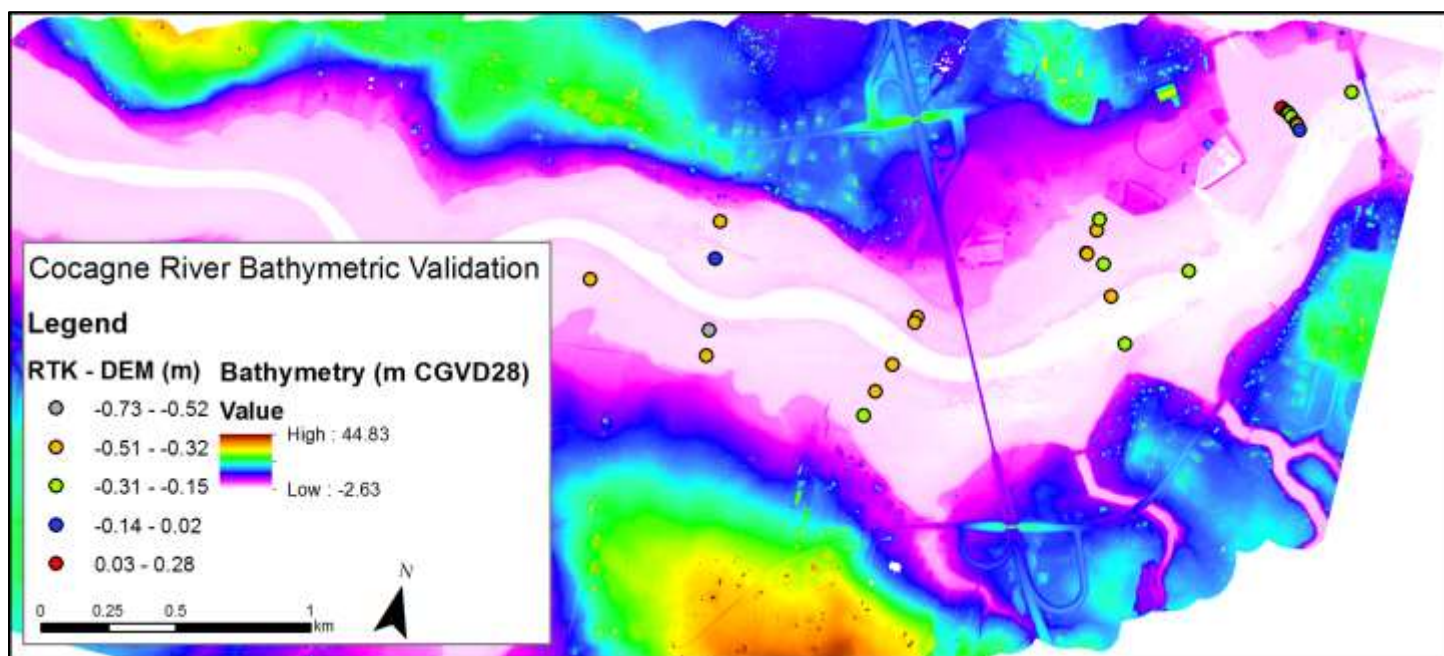


Figure 3.5: Cocagne Bathymetric Validation.

3.2 Surface Models

This section presents Digital Elevation Models (DEMs), Colour Shaded Relief Models, and Depth Normalized Intensity Models for each study area. Each figure in this section includes several sub-panels that focus in on features at a closer scale.

3.2.1 Digital Elevation Models

The Digital Elevation Models for each study area are presented in Figure 3.6 to Figure 3.8. In these figures the minimum and maximum extents of the sub-panels have been adjusted for maximum contrast. Elevation at Saint Simon ranged from 26.6 m elevation on land to a minimum seabed elevation of -5.1 m CGVD28 near the edges of the channel (Figure 3.6). The bathymetric laser did not penetrate the deepest portions of the channel; even the where the river enters the bay in the north (Figure 3.6, aqua sub-panel) we see that the channel is missing. The yellow sub-panel reveals an area that was perhaps dredged to allow boats to access the channel.

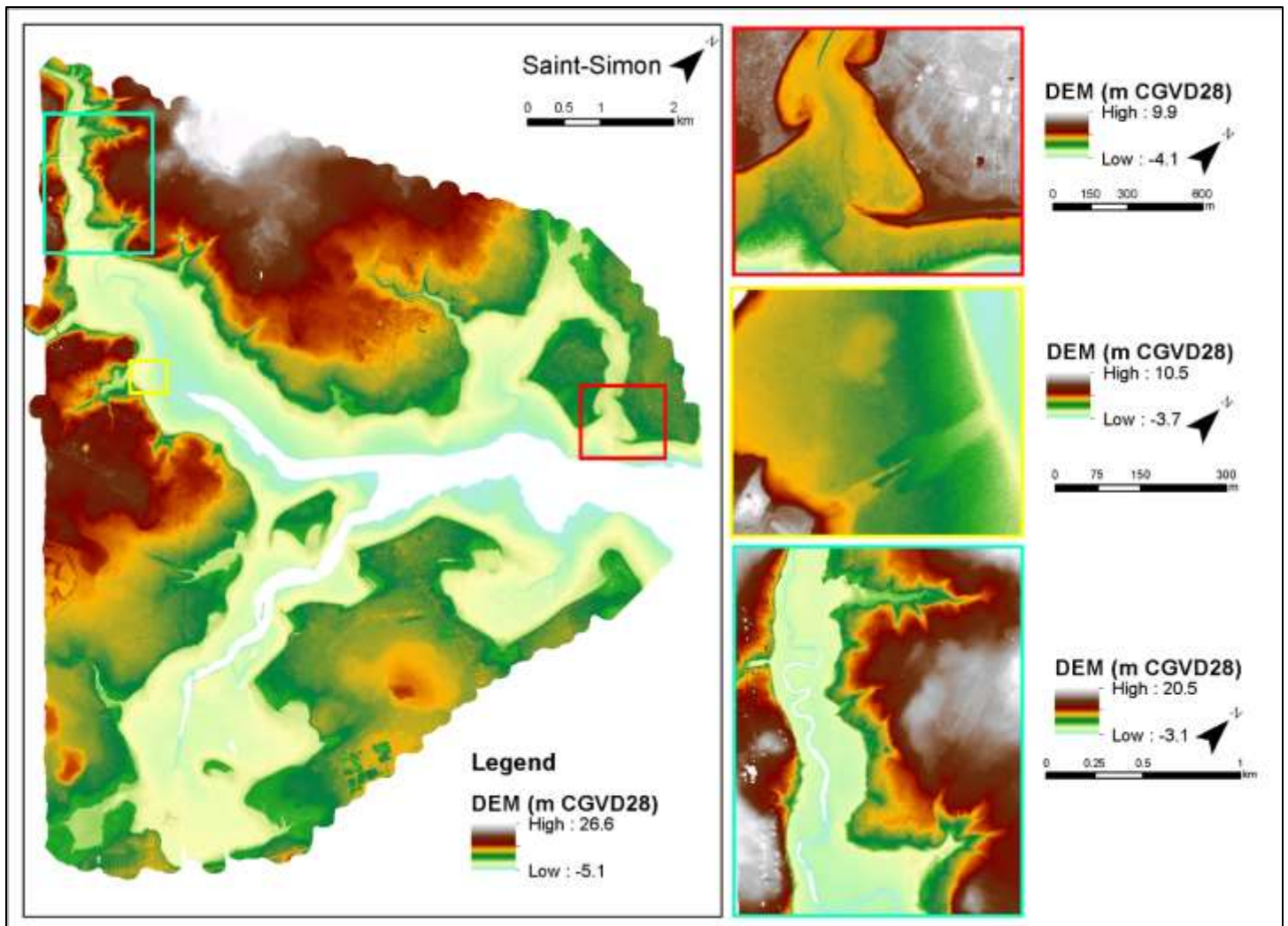


Figure 3.6: Saint Simon Digital Elevation Model for entire study area and insets beside which are matched to the larger figure by border colour.

Topo-Bathymetric Lidar and Photographic Survey of Various Bays located in NB, NS, and PEI

At Tabusintac, the DEM is a synthesis of the two surveys (Oct. 26 and Nov 10). Recall that the first survey on Oct. 26 covered the entire study area but suffered from poor water quality, and the second survey on Nov. 10 covered only the western portion of the area of interest with improved water quality. The final blended DEM ranges from 20.81 m CD on land to -5.75 m CD at the southeastern extent of the study area, outside of the bay (Figure 3.7). The main channel that extends from the southern portion of Tabusintac bay was not detected by the lidar, but the remainder of the bay was; depths on the western side ranged from -0.2 to 0.8 m CD, and 0 to 1.5 m CD on the shallow eastern side. Both of the inset panels show much greater detail in the bathymetry near the eastern edge of the bay, where channels cut through the shallow, dynamic seabed.

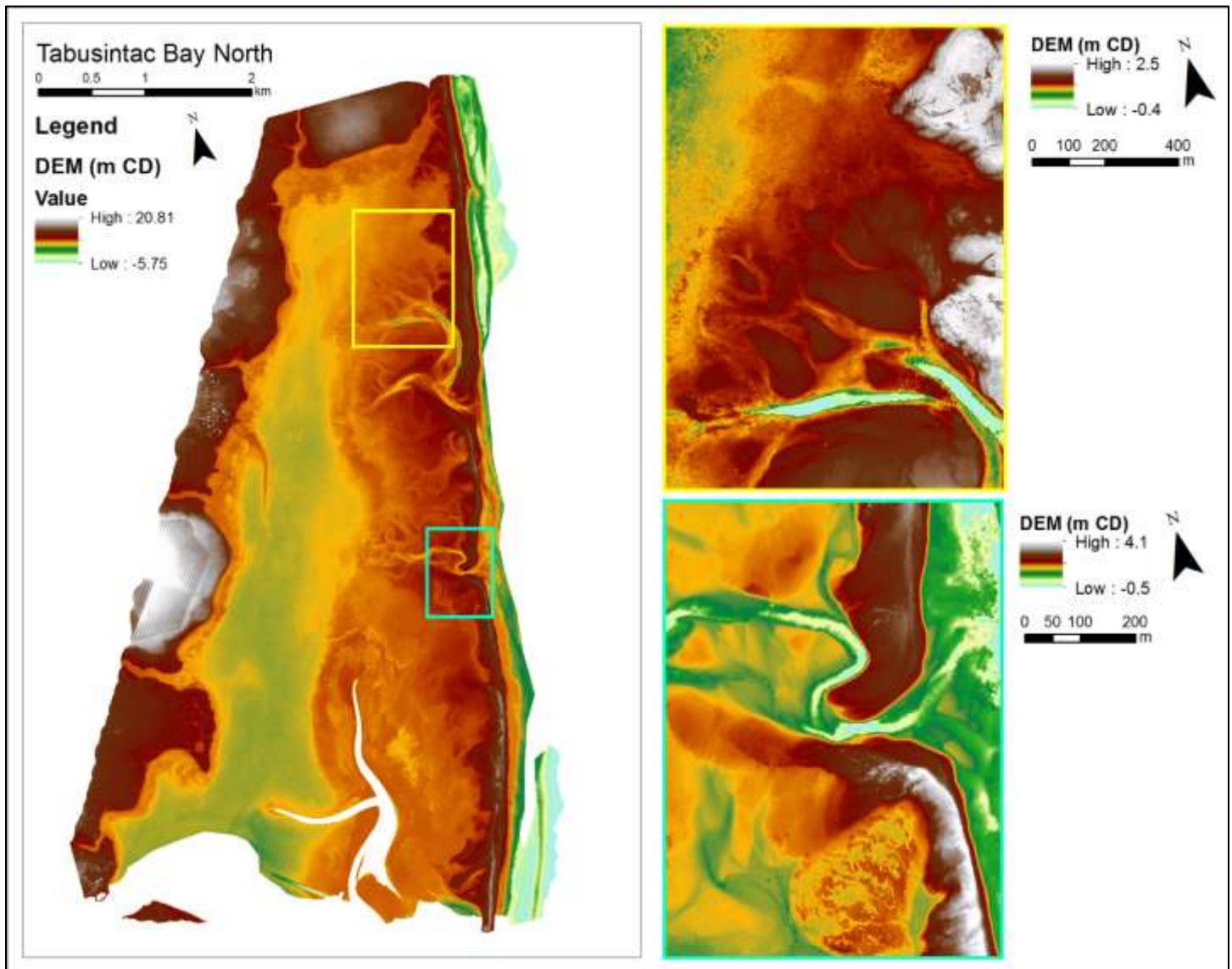


Figure 3.7: Tabusintac Digital Elevation Model for entire study area and insets beside which are matched to the larger figure by border colour. The DEM is a synthesis of the two surveys (Oct. 26 and Nov 10).

Topo-Bathymetric Lidar and Photographic Survey of Various Bays located in NB, NS, and PEI

The Cocagne River DEM ranged from 42.5 m on land to -2.6 m CGVD28 in the water (Figure 3.8). As in the other study sites, the channel was not penetrated by the lidar but coverage elsewhere was excellent, revealing a mostly flat region surrounding the main river channel. The inset panels show river braiding upstream (aqua inset), a shallow bay in the southern region of the study area (yellow inset), and the main highway bridge over the widest portion of the channel (red inset).

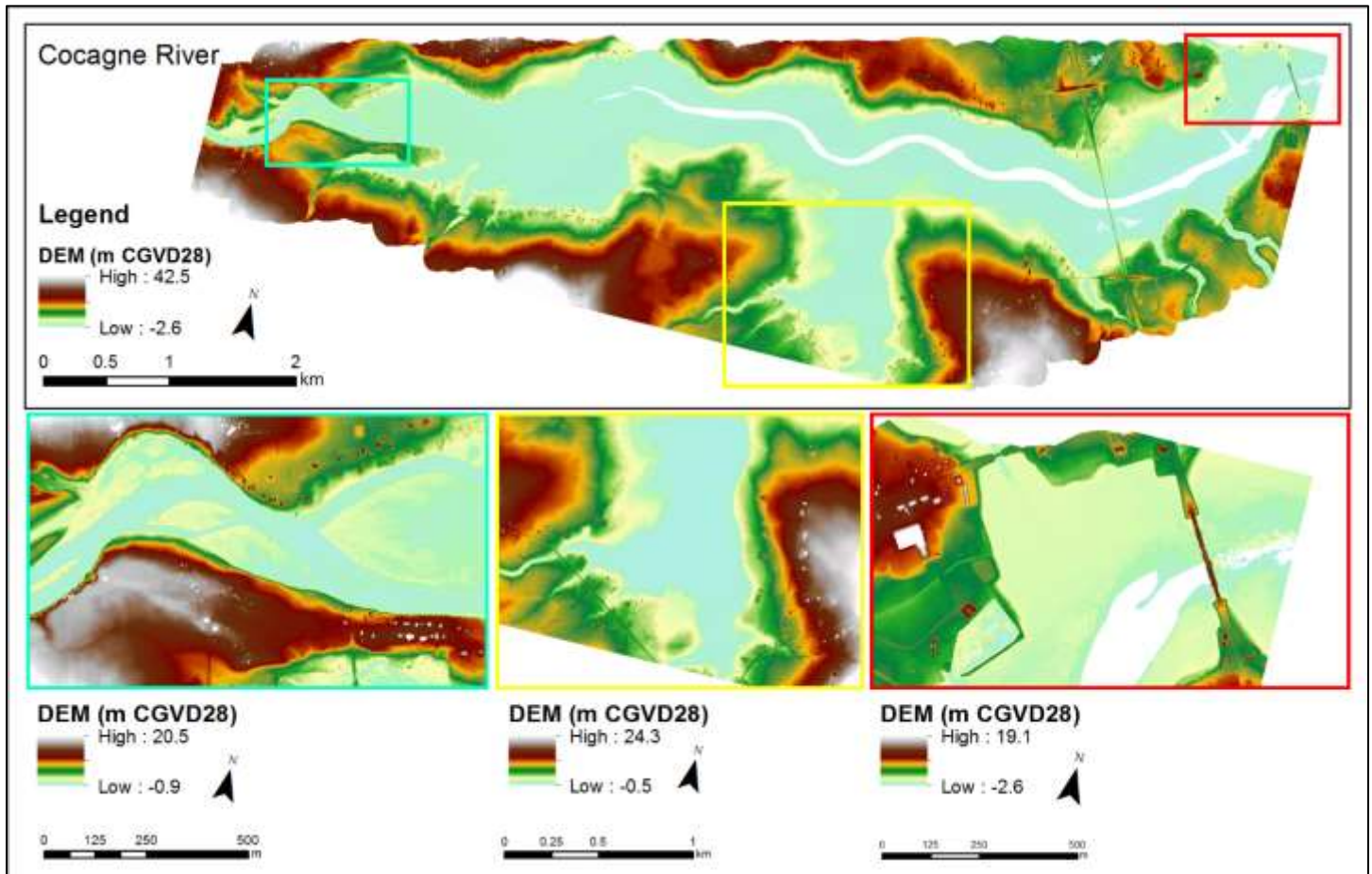


Figure 3.8: Cocagne River Digital Elevation Model for entire study area and insets beside which are matched to the larger figure by border colour.

3.2.2 Colour Shaded Relief Models

The Colour Shaded Relief Models (CSRs) presented in Figure 3.9 to Figure 3.11 show mainly the same features highlighted in the DEMs (Figure 3.6 to Figure 3.8), but the shadow effect accentuates the features differently, allowing more details to be examined. The CSRs are built on the DEMs rather than the DSMs, and use a standard colour scale for the land and a custom colour scale for the bathymetry; 0 m CGVD28 marks the break between land (shades of green for lowlands and red for higher elevations) and ocean (shades of blue, deeper means darker). At Saint Simon (Figure 3.9) the red inset highlights the way the seabed morphology near the protruding spits, provides more detail on the nature of the subsea dredging (yellow inset) and clearly identifies where the lidar penetrated to the river channel and where it missed (aqua

Topo-Bathymetric Lidar and Photographic Survey of Various Bays located in NB, NS, and PEI inset). The Tabusintac CSR emphasizes the different textures in the seabed, where some areas appear very smooth and others fairly rough (Figure 3.10). The CSR products distinguish land and ocean more clearly than the DEM images, showing the exposed land in the river clearly at Cocagne River (Figure 3.11, aqua inset).

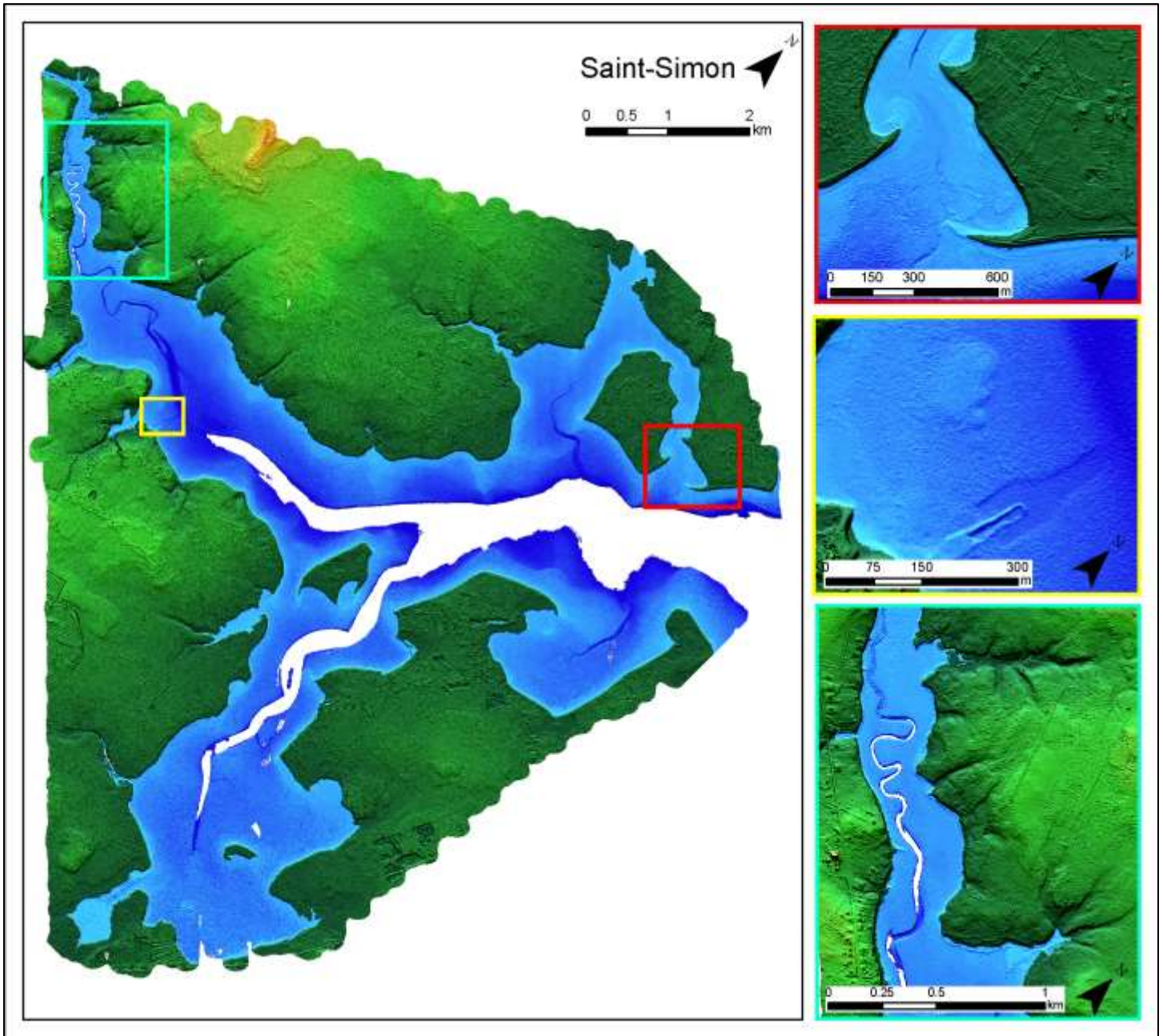


Figure 3.9: Saint-Simon Bay bare-earth Colour Shaded Relief Model showing the whole study area, and insets beside which are matched to the larger figure by border colour.

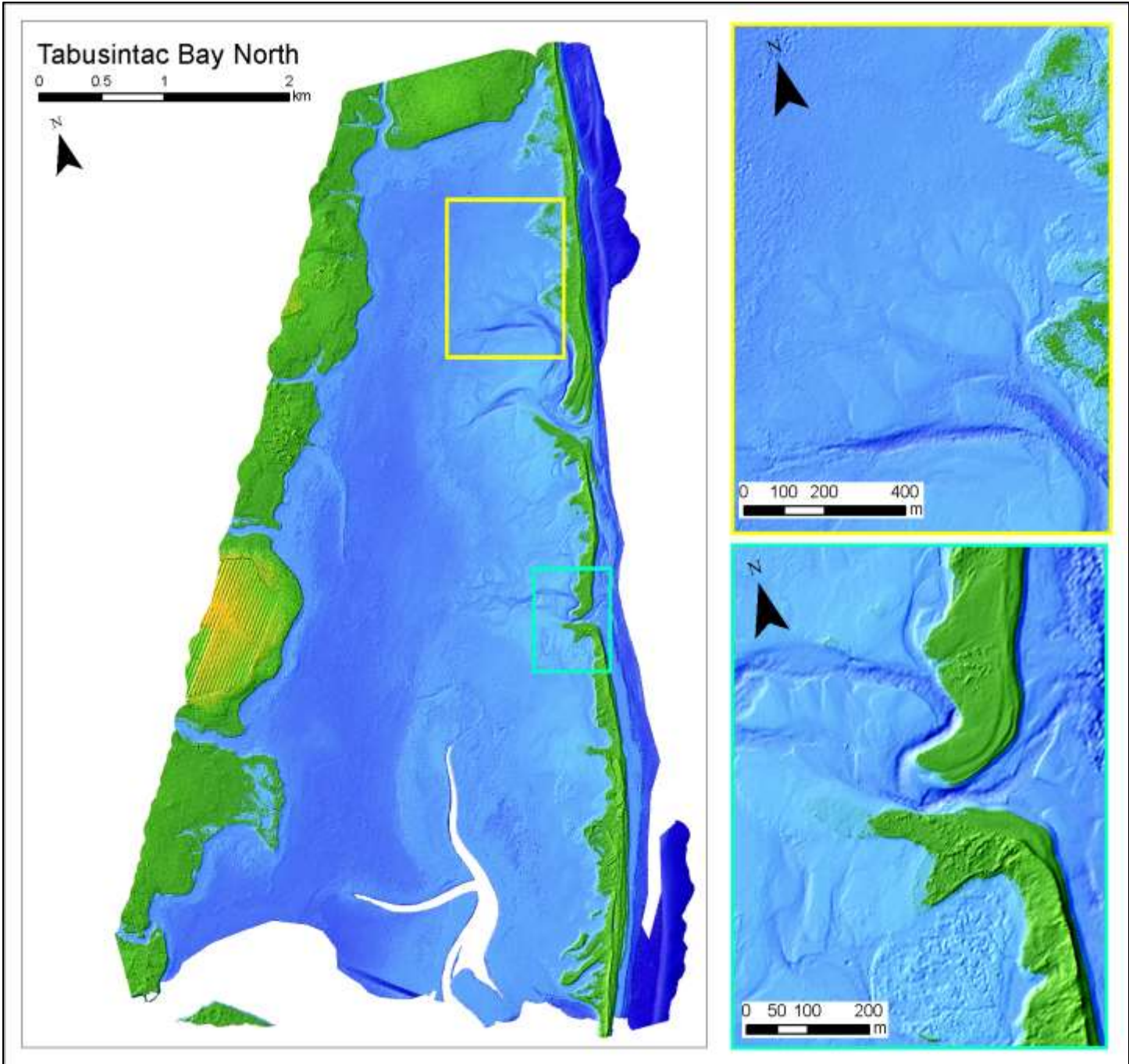


Figure 3.10: Tabusintac Bay bare-earth North Colour Shaded Relief Model showing the whole study area, and insets beside which are matched to the larger figure by border colour.

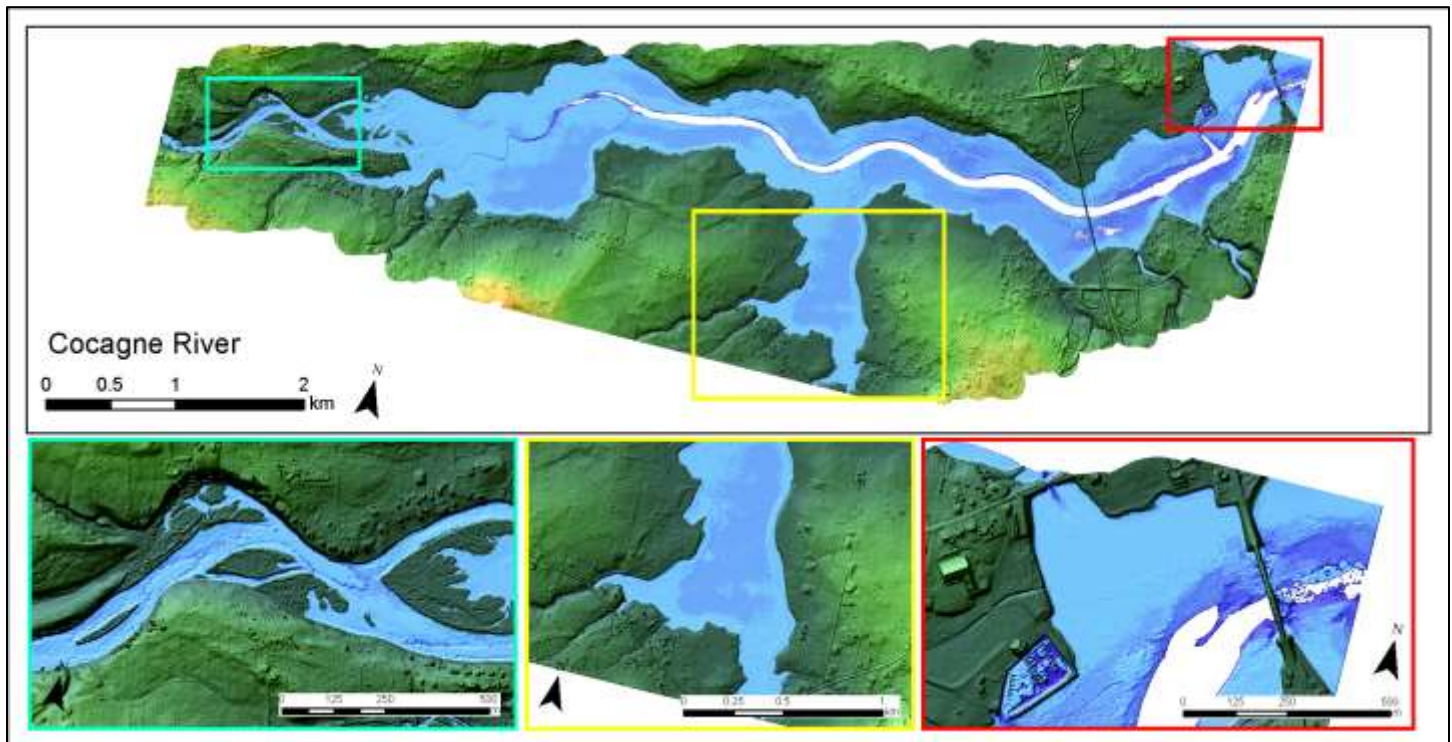


Figure 3.11: Cocagne River bare-earth Colour Shaded Relief Model showing the whole study area, and insets below which are matched to the larger figure by border colour.

3.2.3 Normalized Intensity Models

The depth normalized intensity models (DNIs) can be a powerful tool to reveal submerged features and bottom type information that the air photos and DEM may not show. The amplitude data also show a great deal of contrast between brightly coloured seabed and the dark colour of eelgrass. At Saint-Simon, this contrast is shown clearly in the red and yellow insets (Figure 3.12), while the aqua-coloured inset shows floating aquaculture cages on the left of the image, and submerged cages on the right. The intensity signal is slightly different for the floating and submerged cages, but the air photos confirm which are floating and which are submerged in Figure 3.15. In other cases, the submerged cages are not visible at all in the air photos, but can be identified using the DNI image. At Tabusintac and Cocagne River, vegetation and interesting bottom features are revealed in the intensity data (Figure 3.13 and Figure 3.14, respectively).

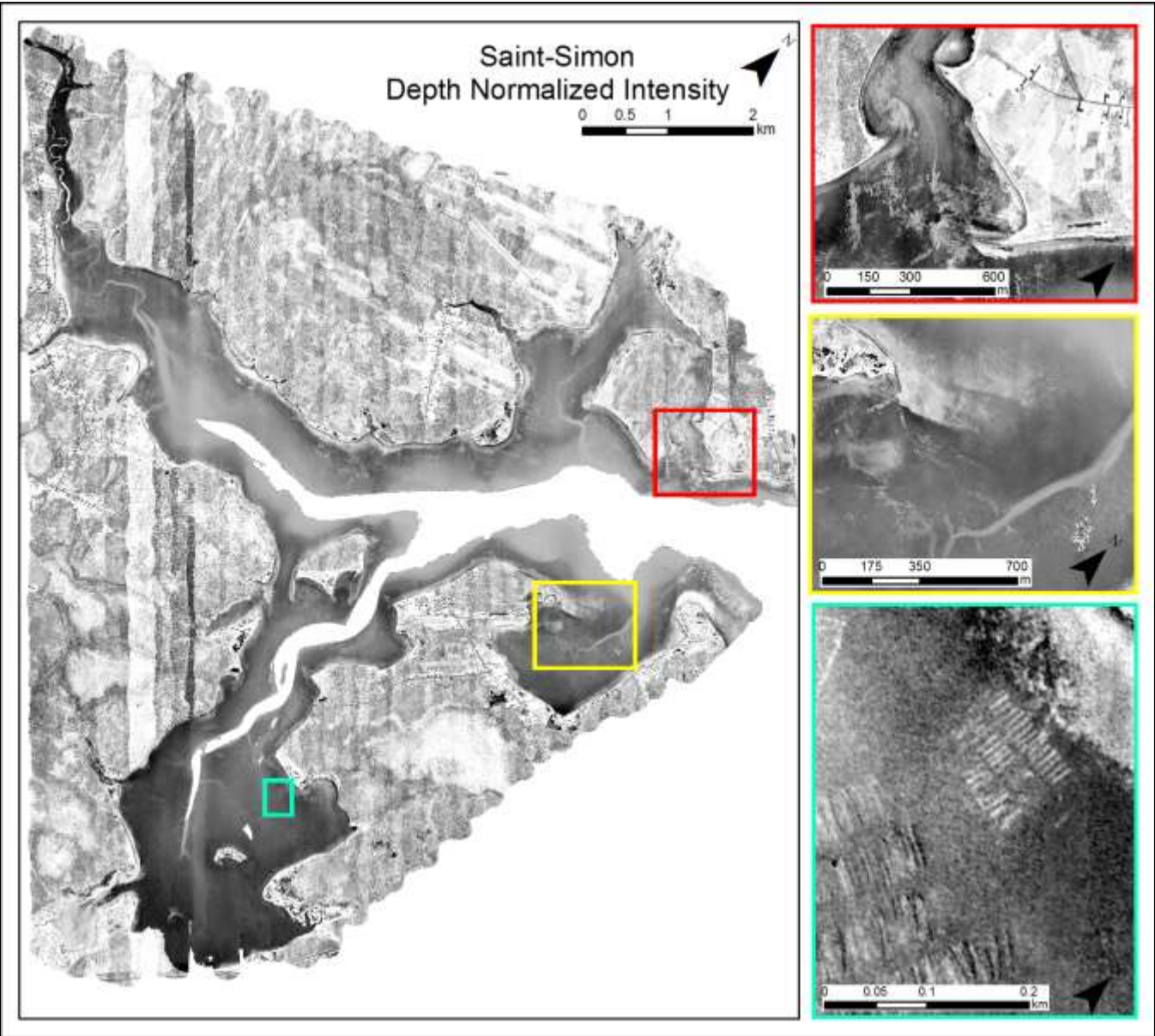


Figure 3.12: Depth normalized intensity/amplitude for Saint-Simon, Oct. 24. The insets on the right correspond to boxes of matching colour on the large map. The red and yellow insets highlight the different intensity signal for submerged eelgrass and sand, while the aqua inset shows floating (on the left) and submerged (on the right) aquaculture cages (the orthophoto for this panel is shown in Figure 3.15).

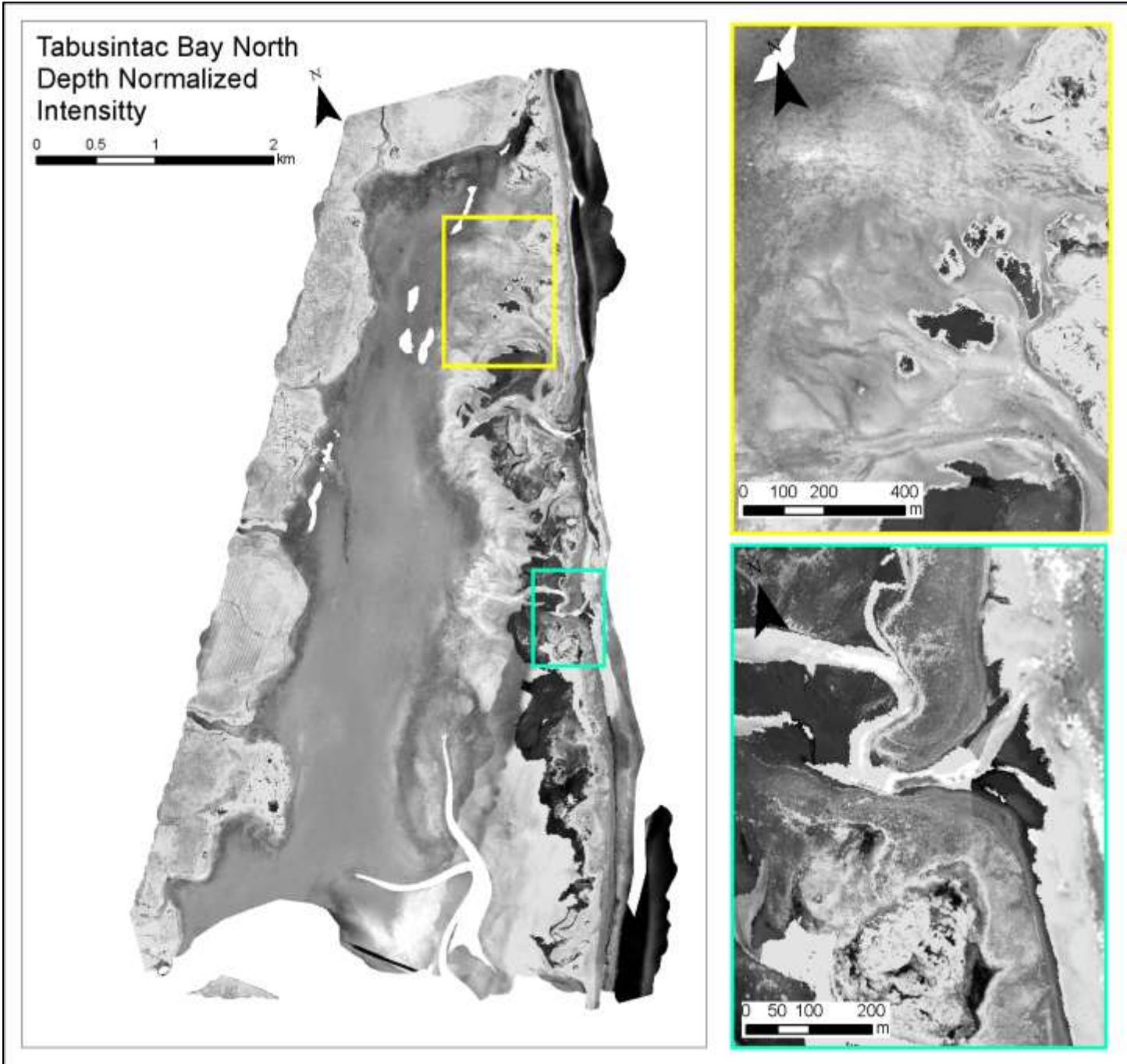


Figure 3.13: Depth normalized intensity/amplitude for Tabusintac. The insets on the right correspond to boxes of matching colour on the large map. The DNI is a synthesis of the two surveys (Oct. 26 and Nov 10).

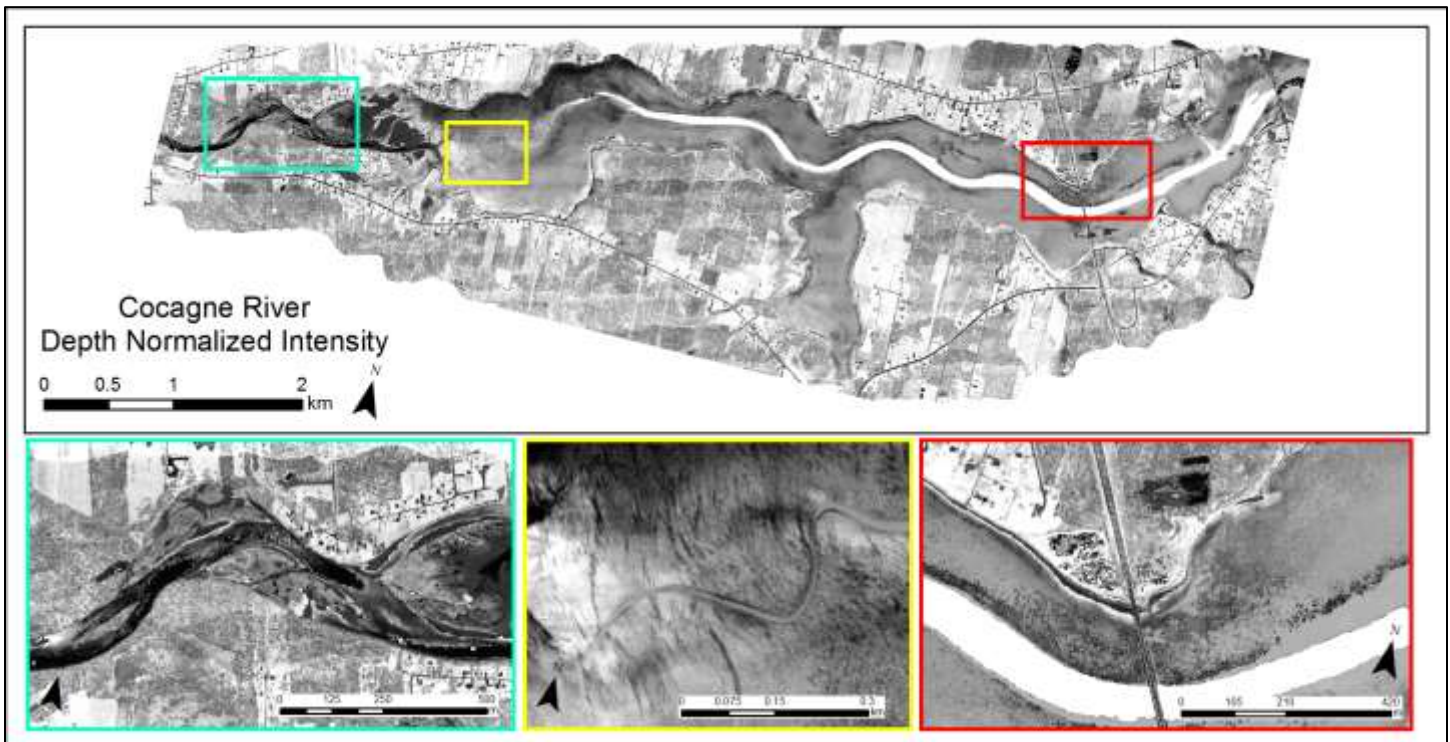


Figure 3.14: Depth normalized intensity/amplitude for Cocagne, Oct. 22. The insets on the bottom correspond to boxes of matching colour on the large map.

3.3 Air Photos

The air photo products are presented in Figure 3.15 through Figure 3.18. As discussed, the mosaic generation can be a challenging process, especially during the fall when sun angle is low. However, the high quality and 5 cm resolution of the photos is clear in the sub-panel images. At Saint-Simon, for example, submerged vegetation can be clearly identified in many areas, the AGRG survey vessel was spotted looking for the light sensors, and both floating and submerged aquaculture was detected (Figure 3.15). At Tabusintac, aquaculture was present during the Oct. 26 survey photos (Figure 3.16), but most of it had been removed from the surface by the Nov. 10 survey (Figure 3.17). The Tabusintac photos reveal a great deal about bottom type, and submerged vegetation can be seen in the Cocagne River photos as well (Figure 3.18).

For data delivery the original 16-bit photos were converted to 8-bit, with four bands (red, green, blue, and near infrared). True Colour Composite (TCC) images and Near Infrared (NIR) images were also produced. The TCC images are composed of the red, green and blue bands saved in a JPEG 2000 format, and the NIR images are a composition of the near infrared, green and blue bands, and saved in a JPEG 2000 format. An example of the differences between these images and the typical 5 cm orthophoto at Cocagne shows how the enhanced images (TCC and NIR) provide more contrast and detail than the unenhanced orthophoto (Figure 3.19).



Figure 3.15: Saint-Simon Bay Orthophoto Mosaic from Oct. 24, 2015 showing the whole study area, and insets beside which are matched to the larger figure by border colour. The insets, from top to bottom, highlight submerged vegetation, the AGRG boat conducting ground truth surveys during the survey, and aquaculture, both submerged and floating, in the southern part of the bay (same extent as Figure 3.12).

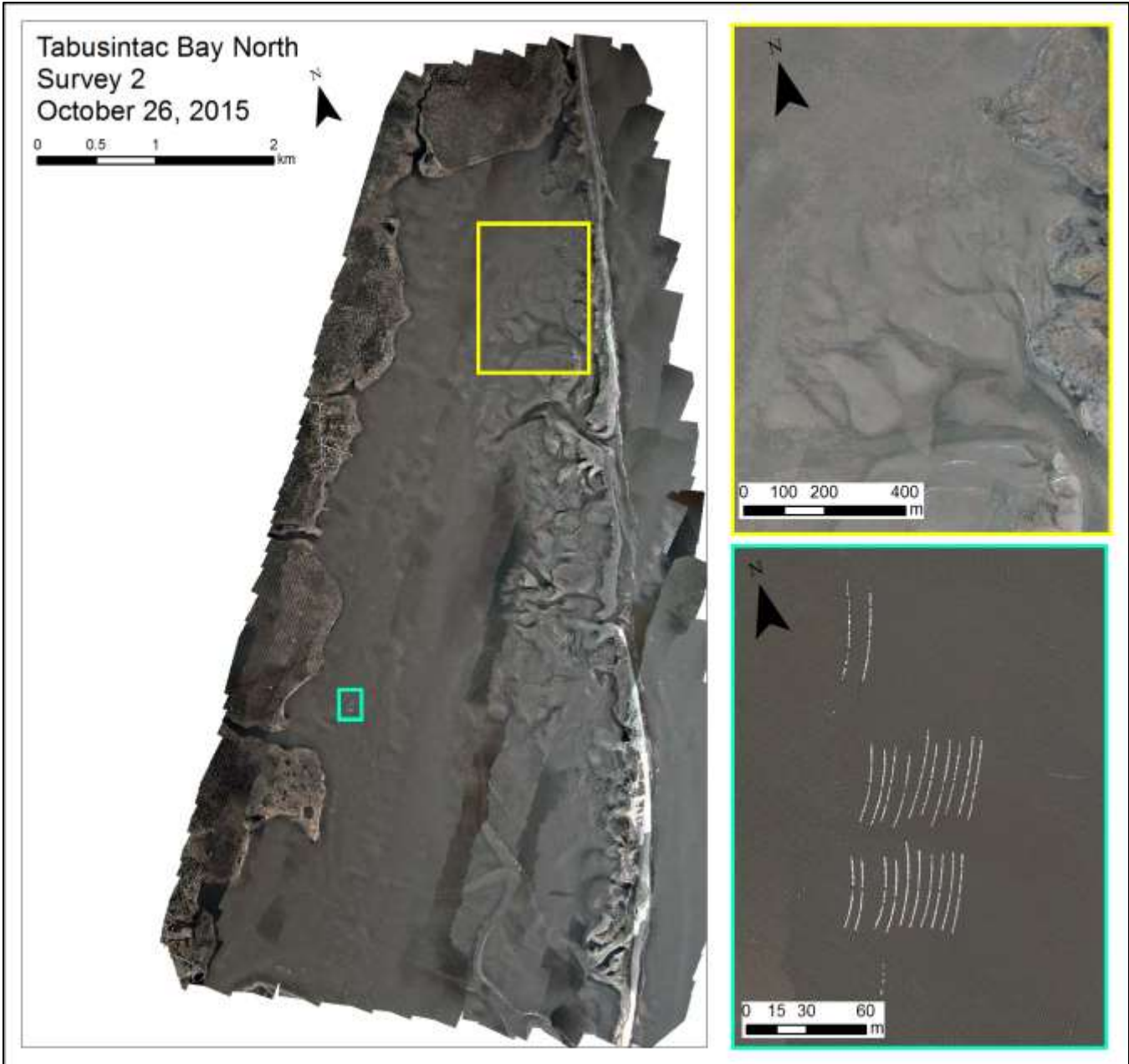


Figure 3.16: Tabusintac Bay North Oct. 26 Orthophoto Mosaic showing the whole study area, and insets beside which are matched to the larger figure by border colour.



Figure 3.17: Tabusintac Bay North Nov. 10 Orthophoto Mosaic showing the whole study area, and insets beside which are matched to the larger figure by border colour. Note the absence of the aquaculture that was visible in Figure 3.16.



Figure 3.18: Cocagne River True Colour Composite Orthophoto Mosaic showing the whole study area, and insets below which are matched to the larger figure by border colour.

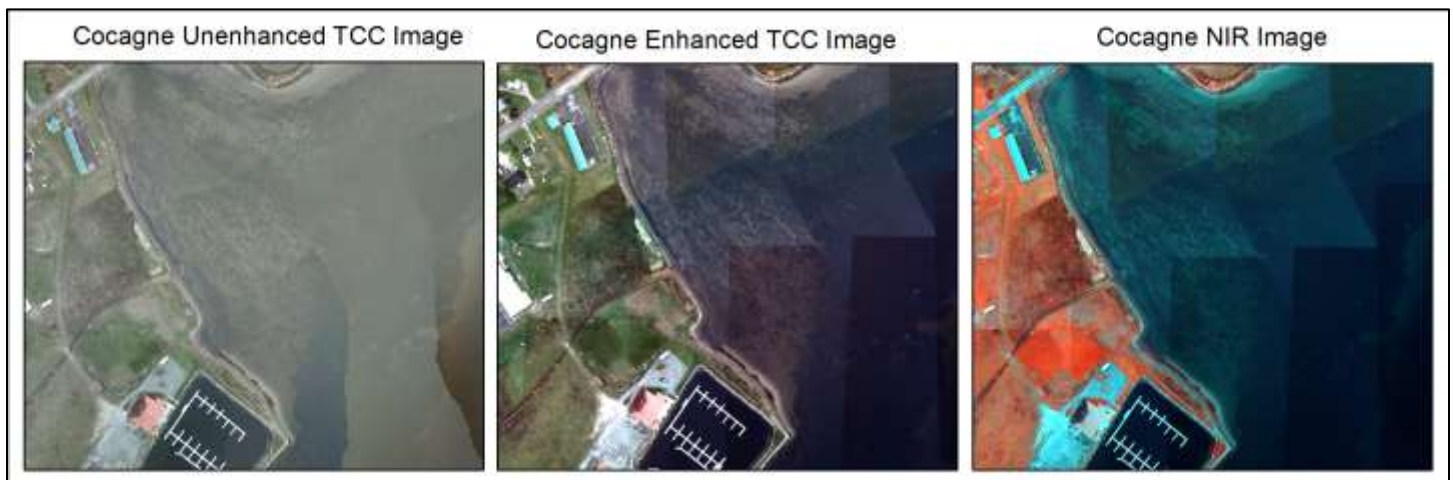


Figure 3.19: Photo products at Cocagne River showing the unenhanced orthophoto mosaic on the left, the enhanced true colour composite in the middle, and the near infrared image on the right. Note how the enhanced images (TCC and NIR) both show the submerged vegetation in much greater contrast and detail than the unenhanced photo.

4 Discussion

4.1 Merging 2014 and 2014 Datasets

The 2014 and 2015 study areas for Tabusintac and Cocagne are shown in Figure 4.1 and Figure 4.2, respectively, and the DEMs for both years are shown in Figure 4.3 and Figure 4.4.

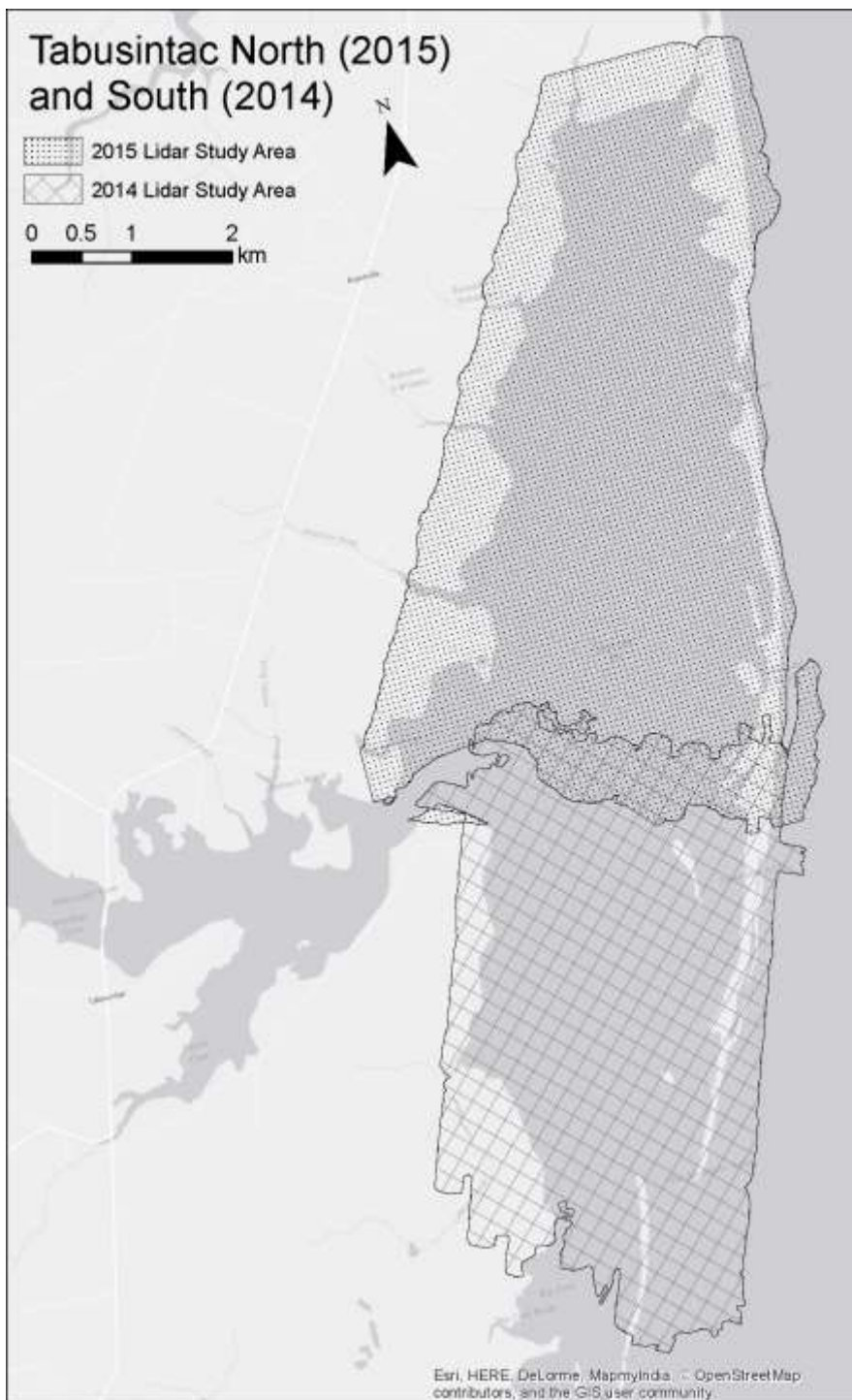


Figure 4.1: Study areas for Tabusintac North, which was surveyed in 2015 for this project, and Tabusintac South, which was surveyed in 2014 for a PWGSC project.

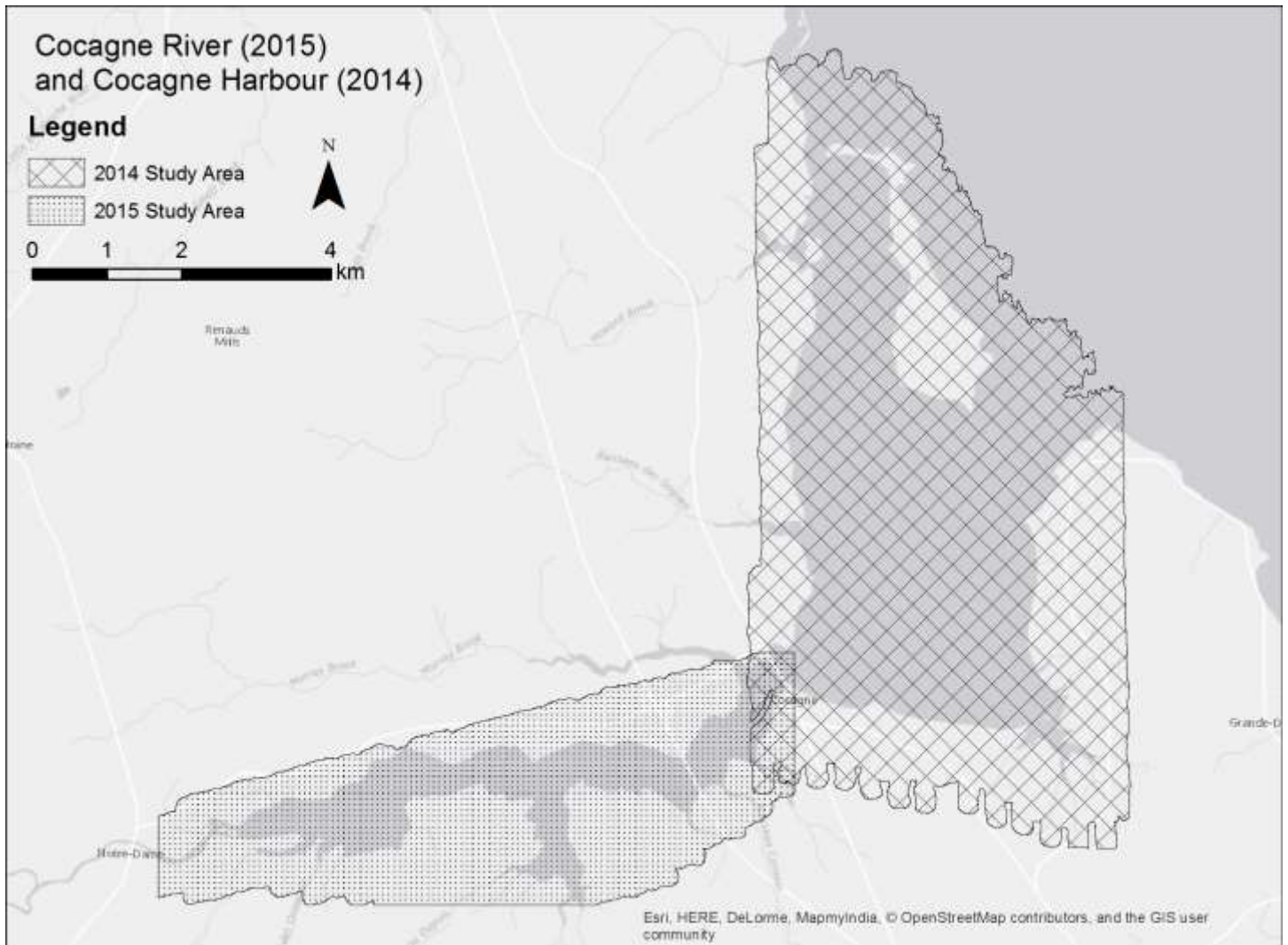


Figure 4.2: Study areas for Cocagne River, which was surveyed in 2015 for this project, and Cocagne Harbour, which was surveyed in 2014, also for DFO Gulf Region.

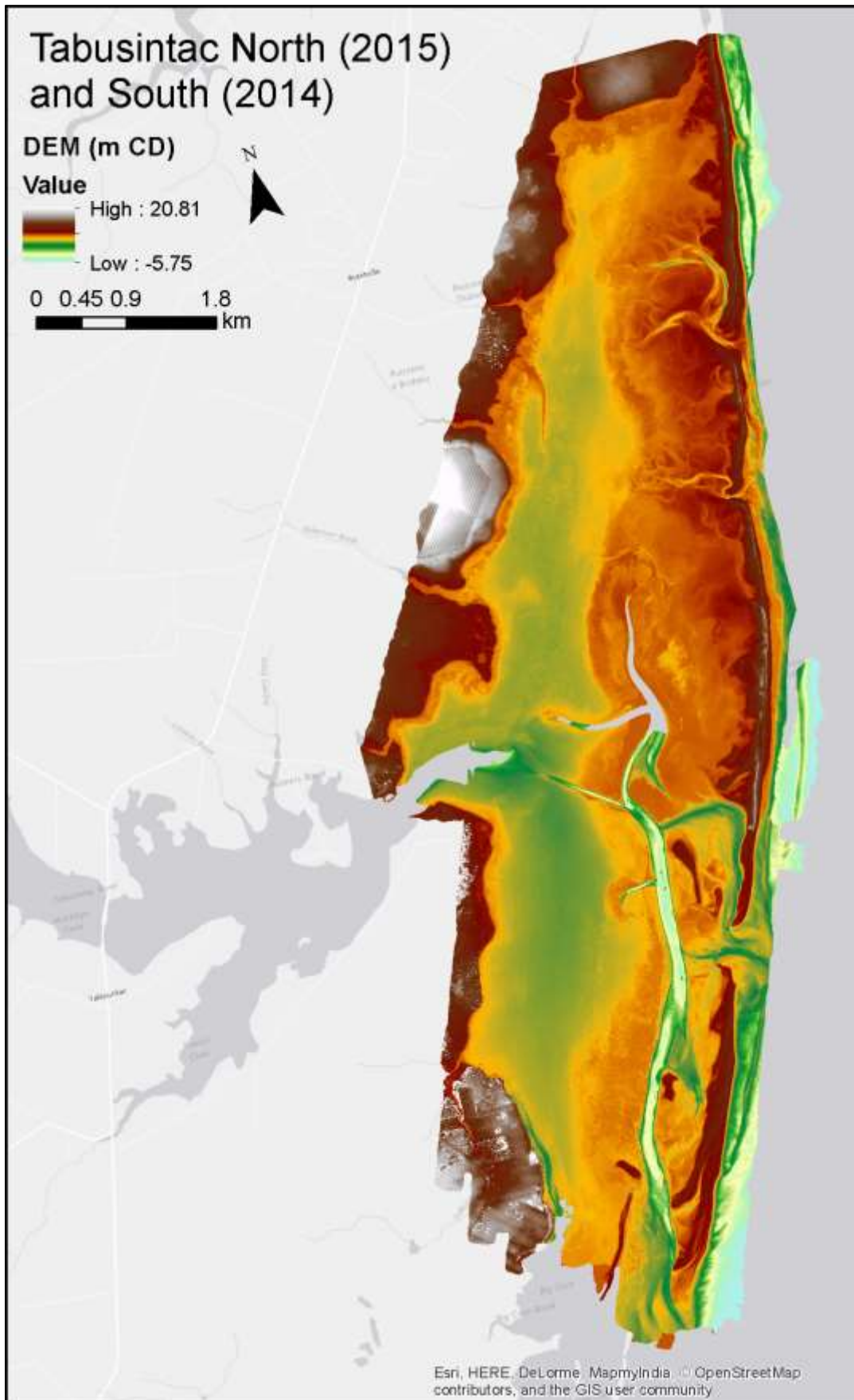


Figure 4.3: Tabusintac North, which was surveyed in 2015 for this project, and Tabusintac South, which was surveyed in 2014 for a PWGSC project.

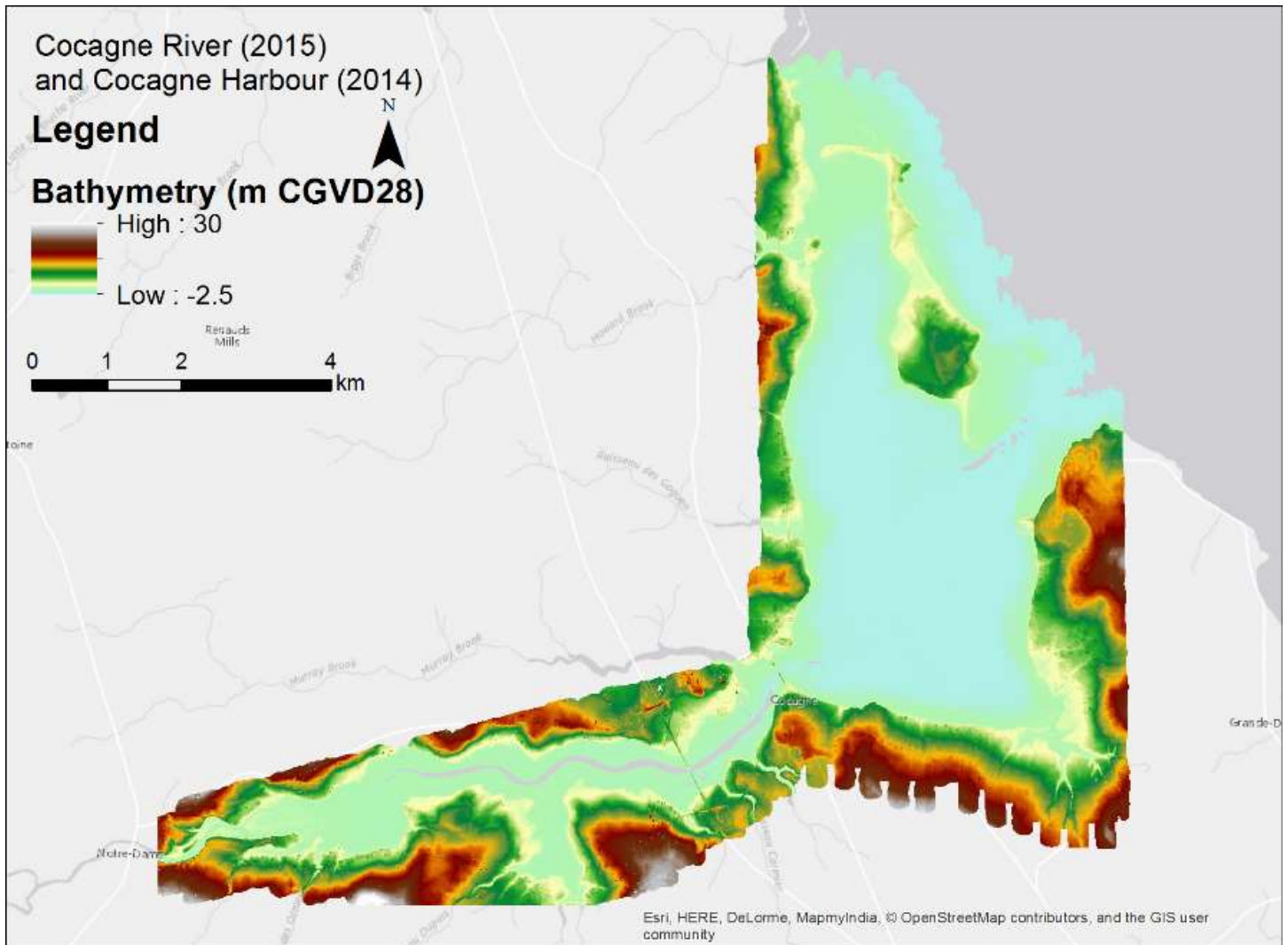


Figure 4.4: Study areas for Cocagne River, which was surveyed in 2015 for this project, and Cocagne Harbour, which was surveyed in 2014, also for DFO Gulf Region.

5 Conclusions

Topographic-bathymetric lidar and photographic surveys were conducted Saint-Simon, Tabusintac North, and Cocagne River, NB, in October and November of 2015. The Tabusintac North and Cocagne River surveys built upon existing lidar surveys from 2014. Digital Elevation Models (DEMs), Digital Surface Models (DSMs), Colour Shaded Relief models (CSRs), Depth Normalized Intensity models (DNI), and orthorectified aerial photograph mosaics were generated for each study site. Lidar collection was successful at all three bays except for the deep channels. Two surveys were required at Tabusintac in order to achieve seabed penetration throughout the study area. Minimum seabed elevations achieved were -5.1 m CGVD28 at Saint-Simon, -5.75 m CD at Tabusintac North, and -2.6 m CGVD28 at Cocagne River. The air photos show floating and submerged aquaculture infrastructure and submerged vegetation at 5 cm resolution. Depth normalized intensity maps that represent bottom type were generated and show sharp contrast between sandy and

Topo-Bathymetric Lidar and Photographic Survey of Various Bays located in NB, NS, and PEI vegetated seabed. Additionally, the intensity maps show submerged aquaculture that is not visible in the air photos. Time of flight ground truth surveys at each study site were conducted to obtain underwater photographs, depth and water clarity measurements.

6 References

Webster, T., McGuigan, K., Crowell, N., Collins, K., and MacDonald, C. in press. Optimization of data collection and refinement of post-processing techniques for Maritime Canada's first shallow water topographic-bathymetric lidar survey In: Roberts, T.M., Rosati, J.D., and Wang, P. (eds.), *Advances in Topobathymetric Mapping, Models, and Applications*. Journal of Coastal Research, Special Issue.

7 Acknowledgements

We would like to thank scientists at DFO Moncton for their support and the Government of Canada for funding support. We would especially like to thank Matt Roscoe, Calvin Gough, Ariel Vallis, Sean Dzafovic and David Kristiansen of NSCC's AGRG for their assistance with collection of ground truth data and data processing for this project. Thanks to staff from Airborne Hydrography and Leica Geosystems and LEG staff for operations support, and AGRG staff for administrative support.

